Tyk2 and Stat3 regulate brown adipose tissue differentiation and obesity.

Elsevier Editorial System(tm) for Cell Metabolism

Manuscript Draft

Manuscript Number: CELL-METABOLISM-D-12-00411R1

Title: Tyk2 and Stat3 Regulate Brown Adipose Tissue Differentiation and Obesity.

Article Type: Research Article

Keywords: JAK/STAT Signaling Pathway; Brown Adipose tissue differentiation; Obesity; A novel role for the tyrosine Kinase Tyk2 and the transcription factor Stat3 in brown fat evelopment

Corresponding Author: Dr. Andrew Charles Larner,

Corresponding Author's Institution: Virginia Commonwelath Unniversity

First Author: Marta Derecka

Order of Authors: Marta Derecka; Agnieszka Gornicka; Sergei B Koralov; Karol Szczepanek; Magdelana Morgan; Vidisha Raje; Jennifer Sisler; Qifang Zhang; Dennis Otero; Joanna Cichy; Klaus Rajewsky; Kazuya Shimoda; Valeria Poli; Birgit Strobl; Sandra Pellegrini; Thurl E Harris; Patrick Seale; Aaron P Russell; Andrew J McAinch; Paul E O'Brien; Susanna R Keller; Colleen M Croniger; Tomasz Kordula; Andrew C Larner, M.D., Ph.D

Abstract: We have made the novel observations that mice lacking the Jak tyrosine kinase member Tyk2 become progressively obese due to aberrant development of Myf5+ brown adipose tissue (BAT). Tyk2 RNA levels in BAT and skeletal muscle, which shares a common progenitor with BAT, are dramatically decreased in mice placed on a high fat diet and in obese humans. Expression of Tyk2 or the constitutively active form of the transcription factor Stat3 (CAStat3) restores differentiation in Tyk2-/- preadipocytes. Furthermore, Tyk2-/- mice expressing CAStat3 transgene in BAT also show improved BAT development, normal levels of insulin and significantly lower body weights. Stat3 binds to PRDM16, a master regulator of BAT differentiation, and enhances the stability of PRDM16 protein. These results define novel roles for Tyk2 and Stat3 as critical determinants of brown fat-lineage and suggest that altered levels of Tyk2 are associated with obesity in both rodents and humans.

Suggested Reviewers:

Opposed Reviewers:

Dear Granger:

I appreciate the opportunity to submit a revised manuscript to Cell Metabolism entitled: **"Tyk2 and Stat3 Regulate Brown Adipose Tissue Differentiation and Obesity".** We have modified the manuscript to include most of the experiments the reviewers suggested. Below I have addressed the reviewer's concerns.

Sincerely,

Andrew Larner

Reviewers' Comments:

Reviewer #1: In a manuscript entitled: "Tyk2 and Stat3 Regulate Brown Adipose Tissue Differentiation and Obesity" Derecka et al. discuss the role of Tyk 2 and Stat3. In general this is an excellent manuscript, the experiments are relevant and carefully executed with the necessary controls. The findings are interesting and important. This reviewer only has a few comments:

The author states that skeletal muscle cells and BAT "originate from the same Myf5 positive progenitor cells, ." the authors should make clear that two different populations of BAT cells exist: the so cold "beige/brite" cells as well as the interscapular or classical BAT cells (e.g. Wu J. et al. Cell 2012 Jul 10). Only classical BAT originates form Myf5 positive precursors whereas beige BAT cells are derived form a different cell population. Even though this is briefly mentioned in the "Discussion" section it should be pointed out already in the abstract. Moreover, it would be of interest to examine whether or not the changes in classical BAT cells described in the ms also are present in beige BAT cells.
We have added a comment in the abstract clarifying our studies were performed in Myf5+ brown adipocytes. We are presently exploring the role of Tyk2 expression in Myf5-negative beige cells. Thus far the results have been inconclusive. The variability in these results may be due to the recently published observation that there are both Myf5+ and Myf5- brown adipocytes in WAT (Sanchez-Gurmaches et al., 2012).

The phenotype observed includes alteration in mRNA levels of genes like ucp1 and a few others as depicted in figures 1F, 4A, 1I. The authors should make sure that the changes in mRNA levels also are reflected by changes in corresponding protein levels using Western blots. Fortunately good commercial antibodies are available for these proteins.
The revised version contains western blots that were used to measure concentrations of proteins depicted in figures 1F and 4A, except PGC1α. We have not located a good commercial antibody that recognizes mouse PGC1α. We observed no increase in levels of UCP1 in Tyk2+/+ BAT with cold exposure (Fig. 1I in previous version and 1J in the revised version). However, changes in the levels

of the protein have been reported to require more than 12 hours exposure to cold (Jacobsson et al., 1994; Klingenspor, 2003).

Fig. 1D shows that in response to high-fat diet Tyk2 mRNA levels are lowered in BAT and SKM whereas no changes could be detected in WAT and liver. The authors should show protein and activity data for Tyk2.
The revised manuscript shows the protein levels of Tyk2 on a normal chow and HFD in BAT and percent decrease of Tyk2 protein in SKM.

Since Tyk2 is regulated in a similar way in both skeletal muscle and iBAT would it be possible that some of the phenotypes observed derive form dysfunction of skeletal muscle cells? Or even a combined general malfunction of mitochondria in SKM and iBAT? This possibility should be discussed more clearly in the ms.
This is an important issue which has been addressed in the discussion in the revised manuscript.

In fig S3B opa1, mfn1 and mfn2 mRNA levels are shown to be lower in Tyk2 -/- mice as compared with wt. This is accompanied with a obese/dysmetabolic phenotype the authors should point out that the reverse i.e. induced levels of opa1, mfn1 and mfn2 has been associated with a "healthy" lean insulin sensitive phenotype, please see Lidell M.E. et al. Diabetes 60:427-35, 2011.
A reference to this paper is in the revised manuscript.

Reviewer #2: This is an interesting study that provides novel insights into the development of brown adipose tissue. The data show an important role for Tyk2 and STAT3 in regulating early events in brown adipocyte formation. Loss of Tyk2 leads to obesity and insulin resistance in mice due most likely to defective BAT activity. These data will be of interest to the readership of Cell Metabolism and will contribute significantly to our understanding of BAT development and the role BAT plays in overall metabolic homeostasis.

Reviewer #3: The manuscript by Derecka et al clearly indicates that global congenital deficiency of Tyk2 results in obesity and some characteristics of diabetes. The results suggest a potential role for Tyk2 in the adipogenesis of brown precursor cells that can be rescued with CASTAT3. There is also data to show an association of PRDM16 and STAT3 that clearly merits further study.

Comments for consideration

The majority of studies indicate that Tyk2 has limited tissue distribution compared to JAKs 1 and 2. What are the levels of Tyk2 in BAT and skeletal muscle (SM) compared to cells where this protein is known to be highly expressed? Are the levels of Tyk2 equivalent in BAT and SM as indicated in Fig. 1D.
Tyk2 is ubiquitously expressed (Strobl et al., 2011). We have included a western

blot showing the levels of the protein in a variety of tissues including SKM, WAT and BAT (Supplemental Fig. S2A). The levels of the protein are increased in BAT compared with SKM.

A limitation to this study is the knockout is global and congenital. The observed metabolic effects could be a result of developmental events. At the least, this issue should be considered in the discussion.
We have commented on this issue in the discussion.

Many references in the text are numerical, but the reference section is by author last name. Hence, it is very difficult to determine source of some information. What is the evidence that tyk2 is the nucleus of BAT?
We have corrected the problem with the references. There is no direct evidence that Tyk2 is in the nucleus of BAT. The report indicating that Tyk2 is in the nucleus used HT1080 cells, which were derived from a human sarcoma. Jak2 was also reported to be in the nucleus in hematopoietic cell lines as well as primary CD34+ stem cells.

What tyk2 and/or STAT3 activators mediate the regulation of key BAT genes like UCP-1 and cidea?
The mediators of Tyk2 need to be delineated. Two possibilities are that Tyk2 phosphorylates Stat3 and other TFs associated with BAT differentiation. However, we have no evidence that Stat3 directly mediates the transcription of BAT-selective genes such as UCP1. Alternatively, Tyk2 may directly or indirectly participate in epigenetic modifications of chromatin involved in expression of BAT-selective genes.

The relevance of the data in Figures 3C and 3D is not clear in the absence of additional studies. An interesting question is whether an interaction of STAT3 and PRDM16 is effected by TZDs. The lack of rosi induced PRDM16 expression is likely because these cells are preadipocytes and do not have any PPARg. The levels of PPARg protein should be shown for the studies in Figures 3C and 3D.
The interaction between Stat3 and PRDM16 is not affected by TZDs. The levels of PPARγ protein are not altered between Stat3+/+ and Stat3-/- (with or without rosiglitazone treatment). Also the induction of PPARγ upon rosiglitazone treatment in preadipocytes is equal between both cell types. This information has been included in the revised Fig. 3E and 3F.

An association of STAT3 and PRDM16 should also be demonstrated by performing the IP with STAT3. Where in the cell is this interaction taking place? Can this interaction be shown without retroviral ectopic expression of PRDM16?
The revised Fig. 3C demonstrates that antibodies to Stat3 immunoprecipitate PRDM16. We also observe the interaction in adipocytes which express endogenous levels of PRDM16 (Fig. 3D). Using extracts prepared from isolated nuclei we have been able to detect an association between Stat3 and PRDM16 (data not shown).

Does Tyk2 activate other STATs besides STAT3? If so, could another STAT also rescue the tyk2 deficiency?

Cytokines that activate Tyk2 also primarily activate Stat3. However, other Stats under selective circumstances can also be activated by Tyk2. We believe it is unlikely that other Stats could rescue the Tyk2 deficiency because, when Stat3 expression is disrupted by shRNA in wild type preadipocytes, these cells do not acquire a brown adipocyte phenotype. These preadipocytes contain all the Stats and Tyk2, which are ubiquitously expressed. If another Stat could replace Stat3, then the preadipocytes should differentiate into functional brown adipocytes

An examination of Tyk2 expression and/or activation in human obesity/T2DM would strengthen the study. In fact, the Materials section describes human subjects, but the data is not in the paper.

The data concerning Tyk2 expression in obese humans is presented in Fig. 1E and supplemental Fig. S2F

The aP2 are no longer considered a strong model for adipocyte expression since aP2 can be expressed in macrophages and the brain. The expression of aP2 in this particular mouse requires investigation**.**

Unfortunately, the analysis of the CAStat3 transgenic mice was initiated prior to the availability of the adiponectin Cre, which expresses in both WAT and BAT. Although the adiponectin Cre has its advantages, the fact that the aP2 Cre randomly expresses in only BAT or WAT has allowed us to exclude the role of WAT in the actions of CAStat3. We have examined bone marrow macrophages from mice that express aP2 Cre and CAStat3 and have not detected expression of CAStat3 in these macrophages. It is possible that CAStat3 is also expressed in the brains of these mice. Assuming mice which express CAStat3 in WAT, also express CAStat3 in brain, one would expect these animals to have a more normal metabolic phenotype than Tyk2-/- mice, if expression of CAStat3 in the brain was contributing to the phenotype. We observe no change in the development of obesity in mice that express CAStat3 in WAT (data not shown). This issue has been addressed in the discussion of the revised manuscript.

The results indicating "The observation that rosiglitazone-induced stabilization of PRDM16 protein is absent in Stat3-/- brown preadipocytes under conditions where there is no change in levels of PRDM16 RNA suggests a new mechanism of Stat3 action' are over interpreted. First, the levels of PPARg are not considered. Secondly, the authors did not examine stabilization of PRDM16; they only examined steady state levels. .

We have modified the original figure (3C and 3D) to include the levels of PPARγ in these immunoblots. We have examined whether the expression of Stat3 controls the rate of degradation of PRDM16 by treating cells with cycloheximide as described by Ohno et al (Ohno et al., 2012). There were no changes in the half-life of PRDM16 protein in Stat3-/- compared to Stat3+/+ adipocytes, suggesting that in these cells the rate of translation of PRDM16 is being influenced by the expression of Stat3. However, these results are difficult to interpret because the endogenous levels of PRDM16 are very low in Stat3-/- cells, which makes difficult to analyze the rates of decay of the protein.

Minor Points:

The data is not published yet, but there is convincing evidence from David Guertin's laboratory that was presented at the ADA meeting that the precursors for BAT and SM is also found in other tissues. Overall, the data indicated that MYRF5 can not be assumed to be a precursor just for BAT and SM. Considering this upcoming data and evident similar observations by other labs, the authors may want to consider rewording some section that indicate 'BAT and skeletal muscle, which shares a common progenitor with BAT." and "Since BAT and skeletal muscles originate from the same Myf5 positive progenitor cells, (8) we conclude that Tyk2 kinase may be important at an early stage of development of these progenitors".
The findings of Guertin's lab have been included in the discussion.

The westerns should contain MW indicators
MW markers are routinely run on SDS page gels, but are not included in the figures.

Jacobsson, A., Muhleisen, M., Cannon, B., and Nedergaard, J. (1994). The uncoupling protein thermogenin during acclimation: indications for pretranslational control. Am J Physiol 267, R999-1007.
Klingenspor, M. (2003). Cold-induced recruitment of brown adipose tissue thermogenesis. Exp Physiol 88, 141-148.
Ohno, H., Shinoda, K., Spiegelman, B.M., and Kajimura, S. (2012). PPARgamma agonists induce a white-to-brown fat conversion through stabilization of PRDM16 protein. Cell Metab 15, 395-404.
Sanchez-Gurmaches, J., Hung, C.M., Sparks, C.A., Tang, Y., Li, H., and Guertin, D.A. (2012). PTEN Loss in the Myf5 Lineage Redistributes Body Fat and Reveals Subsets of White Adipocytes that Arise from Myf5 Precursors. Cell Metab 16, 348-362.
Strobl, B., Stoiber, D., Sexl, V., and Mueller, M. (2011). Tyrosine kinase 2 (TYK2) in cytokine signalling and host immunity. Front Biosci 16, 3214-3232.

Response to Reviewers' Comments:

Reviewer #1: In a manuscript entitled: "Tyk2 and Stat3 Regulate Brown Adipose Tissue Differentiation and Obesity" Derecka et al. discuss the role of Tyk 2 and Stat3. In general this is an excellent manuscript, the experiments are relevant and carefully executed with the necessary controls. The findings are interesting and important. This reviewer only has a few comments:

The author states that skeletal muscle cells and BAT "originate from the same Myf5 positive progenitor cells, ." the authors should make clear that two different populations of BAT cells exist: the so cold "beige/brite" cells as well as the interscapular or classical BAT cells (e.g. Wu J. et al. Cell 2012 Jul 10). Only classical BAT originates form Myf5 positive precursors whereas beige BAT cells are derived form a different cell population. Even though this is briefly mentioned in the "Discussion" section it should be pointed out already in the abstract. Moreover, it would be of interest to examine whether or not the changes in classical BAT cells described in the ms also are present in beige BAT cells.
We have added a comment in the abstract clarifying our studies were performed in myf5+ brown adipocytes. We are presently exploring the role of Tyk2 expression in myf5-negative beige cells. Thus far the results have been inconclusive. The variability in these results may be due to the recently published observation that there are both myf5+ and myf5- brown adipocytes in WAT (Sanchez-Gurmaches et al., 2012).

The phenotype observed includes alteration in mRNA levels of genes like ucp1 and a few others as depicted in figures 1F, 4A, 1I. The authors should make sure that the changes in mRNA levels also are reflected by changes in corresponding protein levels using Western blots. Fortunately good commercial antibodies are available for these proteins.
The revised version contains western blots that were used to measure concentrations of proteins depicted in figures 1F and 4A, except PGC1α. We have not located a good commercial antibody that recognizes mouse PGC1α. We observed no increase in levels of UCP1 in Tyk2+/+ BAT with cold exposure (Fig. 1I in previous version and 1J in the revised version). However, changes in the levels of the protein have been reported to require more than 12 hours exposure to cold (Jacobsson et al., 1994; Klingenspor, 2003).

Fig. 1D shows that in response to high-fat diet Tyk2 mRNA levels are lowered in BAT and SKM whereas no changes could be detected in WAT and liver. The authors should show protein and activity data for Tyk2.
The revised manuscript shows the protein levels of Tyk2 on a normal chow and HFD in BAT and percent decrease of Tyk2 protein in SKM.

Since Tyk2 is regulated in a similar way in both skeletal muscle and iBAT would it be possible that some of the phenotypes observed derive form dysfunction of skeletal muscle cells? Or even a combined general malfunction of mitochondria in SKM and iBAT? This possibility should be discussed more clearly in the ms.
This is an important issue which has been addressed in the discussion in the

revised manuscript.

In fig S3B opa1, mfn1 and mfn2 mRNA levels are shown to be lower in Tyk2 -/- mice as compared with wt. This is accompanied with a obese/dysmetabolic phenotype the authors should point out that the reverse i.e. induced levels of opa1, mfn1 and mfn2 has been associated with a "healthy" lean insulin sensitive phenotype, please see Lidell M.E. et al. Diabetes 60:427-35, 2011.
A reference to this paper is in the revised manuscript.

Reviewer #2: This is an interesting study that provides novel insights into the development of brown adipose tissue. The data show an important role for Tyk2 and STAT3 in regulating early events in brown adipocyte formation. Loss of Tyk2 leads to obesity and insulin resistance in mice due most likely to defective BAT activity. These data will be of interest to the readership of Cell Metabolism and will contribute significantly to our understanding of BAT development and the role BAT plays in overall metabolic homeostasis.

Reviewer #3: The manuscript by Derecka et al clearly indicates that global congenital deficiency of Tyk2 results in obesity and some characteristics of diabetes. The results suggest a potential role for Tyk2 in the adipogenesis of brown precursor cells that can be rescued with CASTAT3. There is also data to show an association of PRDM16 and STAT3 that clearly merits further study.

Comments for consideration

The majority of studies indicate that Tyk2 has limited tissue distribution compared to JAKs 1 and 2. What are the levels of Tyk2 in BAT and skeletal muscle (SM) compared to cells where this protein is known to be highly expressed? Are the levels of Tyk2 equivalent in BAT and SM as indicated in Fig. 1D.
Tyk2 is ubiquitously expressed (Strobl et al., 2011). We have included a western blot showing the levels of the protein in a variety of tissues including SKM, WAT and BAT (Supplemental Fig. S2A). The levels of the protein are increased in BAT compared with SKM.

A limitation to this study is the knockout is global and congenital. The observed metabolic effects could be a result of developmental events. At the least, this issue should be considered in the discussion.
We have commented on this issue in the discussion.

Many references in the text are numerical, but the reference section is by author last name. Hence, it is very difficult to determine source of some information. What is the evidence that tyk2 is the nucleus of BAT?
We have corrected the problem with the references. There is no direct evidence that Tyk2 is in the nucleus of BAT. The report indicating that Tyk2 is in the nucleus

used HT1080 cells which were derived from a human sarcoma. Jak2 was also reported to be in the nucleus in hematopoietic cell lines as well as primary CD34+ stem cells.

What tyk2 and/or STAT3 activators mediate the regulation of key BAT genes like UCP-1 and cidea?
The mediators of Tyk2 need to be delineated. Two possibilities are that Tyk2 phosphorylates Stat3 and other TFs associated with BAT differentiation. However, we have no evidence that Stat3 directly mediates the transcription of BAT-selective genes such as UCP1. Alternatively, Tyk2 may directly or indirectly participate in epigenetic modifications of chromatin involved in expression of BAT-selective genes.

The relevance of the data in Figures 3C and 3D is not clear in the absence of additional studies. An interesting question is whether an interaction of STAT3 and PRDM16 is effected by TZDs. The lack of rosi induced PRDM16 expression is likely because these cells are preadipocytes and do not have any PPARg. The levels of PPARg protein should be shown for the studies in Figures 3C and 3D.
The interaction between Stat3 and PRDM16 is not affected by TZDs. The levels of PPARγ protein are not altered between Stat3+/+ and Stat3-/- (with or without rosiglitazone treatment). Also the induction of PPARγ upon rosiglitazone treatment in preadipocytes is equal between both cell types. This information has been included in the revised Fig. 3E and 3F.

An association of STAT3 and PRDM16 should also be demonstrated by performing the IP with STAT3. Where in the cell is this interaction taking place? Can this interaction be shown without retroviral ectopic expression of PRDM16?
The revised Fig. 3C demonstrates that antibodies to Stat3 immunoprecipitate PRDM16. We also observe the interaction in adipocytes which express endogenous levels of PRDM16 (Fig. 3D). Using extracts prepared from isolated nuclei we have been able to detect an association between Stat3 and PRDM16 (data not shown).

Does Tyk2 activate other STATs besides STAT3? If so, could another STAT also rescue the tyk2 deficiency?
Cytokines that activate Tyk2 also primarily activate Stat3. However, other Stats under selective circumstances can also be activated by Tyk2. We believe it is unlikely that other Stats could rescue the Tyk2 deficiency because, when Stat3 expression is disrupted by shRNA in wild type preadipocytes, these cells do not acquire a brown adipocyte phenotype. These preadipocytes contain all the Stats and Tyk2, which are ubiquitously expressed. If another Stat could replace Stat3, then the preadipocytes should differentiate into functional brown adipocytes

An examination of Tyk2 expression and/or activation in human obesity/T2DM would strengthen the study. In fact, the Materials section describes human subjects, but the data is not in the paper.
The data concerning Tyk2 expression in obese humans is presented in Fig. 1E and

supplemental Fig. S2F

The aP2 are no longer considered a strong model for adipocyte expression since aP2 can be expressed in macrophages and the brain. The expression of aP2 in this particular mouse requires investigation**.**
Unfortunately, the analysis of the CAStat3 transgenic mice was initiated prior to the availability of the adiponectin Cre, which expresses in both WAT and BAT. Although the adiponectin Cre has its advantages, the fact that the aP2 Cre randomly expresses in only BAT or WAT has allowed us to exclude the role of WAT in the actions of CAStat3. We have examined bone marrow macrophages from mice that express aP2 Cre and CAStat3 and have not detected expression of CAStat3 in these macrophages. It is possible that CAStat3 is also expressed in the brains of these mice. Assuming mice which express CAStat3 in WAT, also express CAStat3 in brain, one would expect these animals to have a more normal metabolic phenotype than Tyk2-/- mice, if expression of CAStat3 in the brain was contributing to the phenotype. We observe no change in the development of obesity in mice that express CAStat3 in WAT (data not shown). This issue has been addressed in the discussion of the revised manuscript.

The results indicating "The observation that rosiglitazone-induced stabilization of PRDM16 protein is absent in Stat3-/- brown preadipocytes under conditions where there is no change in levels of PRDM16 RNA suggests a new mechanism of Stat3 action' are over interpreted. First, the levels of PPARg are not considered. Secondly, the authors did not examine stabilization of PRDM16; they only examined steady state levels. .
We have modified the original figure (3C and 3D) to include the levels of PPARγ in these immunoblots. We have examined whether the expression of Stat3 controls the rate of degradation of PRDM16 by treating cells with cycloheximide as described by Ohno et al (Ohno et al., 2012). There were no changes in the half-life of PRDM16 protein in Stat3-/- compared to Stat3+/+ adipocytes, suggesting that in these cells the rate of translation of PRDM16 is being influenced by the expression of Stat3. However, these results are difficult to interpret because the endogenous levels of PRDM16 are very low in Stat3-/- cells, which makes difficult to analyze the rates of decay of the protein.

Minor Points:

The data is not published yet, but there is convincing evidence from David Guertin's laboratory that was presented at the ADA meeting that the precursors for BAT and SM is also found in other tissues. Overall, the data indicated that MYRF5 can not be assumed to be a precursor just for BAT and SM. Considering this upcoming data and evident similar observations by other labs, the authors may want to consider rewording some section that indicate 'BAT and skeletal muscle, which shares a common progenitor with BAT." and "Since BAT and skeletal muscles originate from the same Myf5 positive progenitor cells, (8) we conclude that Tyk2 kinase may be important at an early stage of development of these progenitors".
The findings of Guertin's lab have been included in the discussion.

The westerns should contain MW indicators
MW markers are routinely run on SDS page gels, but are not included in the figures.

Jacobsson, A., Muhleisen, M., Cannon, B., and Nedergaard, J. (1994). The uncoupling protein thermogenin during acclimation: indications for pretranslational control. Am J Physiol 267, R999-1007.
Klingenspor, M. (2003). Cold-induced recruitment of brown adipose tissue thermogenesis. Exp Physiol 88, 141-148.
Ohno, H., Shinoda, K., Spiegelman, B.M., and Kajimura, S. (2012). PPARgamma agonists induce a white-to-brown fat conversion through stabilization of PRDM16 protein. Cell Metab 15, 395-404.
Sanchez-Gurmaches, J., Hung, C.M., Sparks, C.A., Tang, Y., Li, H., and Guertin, D.A. (2012). PTEN Loss in the Myf5 Lineage Redistributes Body Fat and Reveals Subsets of White Adipocytes that Arise from Myf5 Precursors. Cell Metab 16, 348-362.
Strobl, B., Stoiber, D., Sexl, V., and Mueller, M. (2011). Tyrosine kinase 2 (TYK2) in cytokine signalling and host immunity. Front Biosci 16, 3214-3232.

Tyk2 and Stat3 Regulate Brown Adipose Tissue Differentiation and Obesity.

Marta Derecka[1,], Agnieszka Gornicka[2,], Sergei B. Koralov[3], Karol Szczepanek[1,6], Magdalena Morgan[1], Vidisha Raje[1], Jennifer Sisler[1], Qifang Zhang[1], Dennis Otero[4], Joanna Cichy[5], Klaus Rajewsky[3], Kazuya Shimoda[7], Valeria Poli[8], Birgit Strobl[9], Sandra Pellegrini[10], Thurl E. Harris[11], Patrick Seale[12], Aaron P. Russell[13], Andrew J. McAinch[14], Paul E. O'Brien[15] Susanna R. Keller[16], Colleen M. Croniger[17], Tomasz Kordula[1], and Andrew C. Larner[1,18].

[1] Department of Biochemistry and Molecular Biology, and Massey Cancer Center, Virginia Commonwealth University, Richmond, VA 23298, USA

[2] Department of Immunology Cleveland Clinic Foundation, Cleveland, OH 44195, USA

[3] CBR Institute for Biomedical Research, Harvard Medical School, Boston, MA 02115, USA

[4] Division of Biological Sciences, University of California, San Diego, La Jolla, CA 92093, USA

[5] Department of Immunology, Faculty of Biochemistry, Biophysics and Biotechnology, Jagiellonian University, Krakow, Poland

[6] Department of Medical Biotechnology, Faculty of Biochemistry, Biophysics, and Biotechnology, Jagiellonian University, Krakow, Poland

[7] Department of Gastroenterology and Hematology, Faculty of Medicine, Miyazaki University, Japan

[8] Department of Genetics, Biology and Biochemistry, Molecular Biotechnology Center University of Turin, Via Nizza 52, 10126 Torino Italy

[9] Institute of Animal Breeding and Genetics, University of Veterinary Medicine Vienna, Austria

[10] Department of Immunology, Institut Pasteur, 25, 28 rue du Docteur Roux 75724 Paris, France

[11] Department of Pharmacology, University of Virginia School of Medicine, Charlottesville, VA, 22903, USA

[12] Department of Cell and Developmental Biology, University of Pennsylvania School of Medicine, Philadelphia, PA, 19104, USA

[13] Centre of Physical Activity and Nutrition (C-PAN) Research, School of Exercise and Nutrition Sciences, Deakin University, Burwood, 3125, Australia

[14] Biomedical and Lifestyle Diseases (BioLED) Unit, School of Biomedical and Health Sciences, Victoria University, St Albans, 3021, Australia

[15] Centre for Obesity Research and Education (CORE), Monash University, The Alfred Hospital, Melbourne, 3004, Australia

[16] Department of Medicine, University of Virginia School of Medicine, Charlottesville, VA 22908, USA

[17] Department of Nutrition, Case Western University School of Medicine Cleveland, OH 44106, USA

[18] To whom correspondence should be addressed. Tel. (804) 828-2903; Fax: (804) 827-1657; Email: alarner@vcu.ed

Abstract

We have made the novel observations that mice lacking the Jak tyrosine kinase member Tyk2 become progressively obese due to aberrant development of Myf5+ brown adipose tissue (BAT). Tyk2 RNA levels in BAT and skeletal muscle, which shares a common progenitor with BAT, are dramatically decreased in mice placed on a high fat diet and in obese humans. Expression of Tyk2 or the constitutively active form of the transcription factor Stat3 (CAStat3) restores differentiation in Tyk2-/- brown preadipocytes. Furthermore, Tyk2-/- mice expressing CAStat3 transgene in BAT also show improved BAT development, normal levels of insulin and significantly lower body weights. Stat3 binds to PRDM16, a master regulator of BAT differentiation, and enhances the stability of PRDM16 protein. These results define novel roles for Tyk2 and Stat3 as critical determinants of brown fat-lineage and suggest that altered levels of Tyk2 are associated with obesity in both rodents and humans.

Introduction

Obesity occurs when caloric intake exceeds energy expenditure with excess nutrients stored as fat. There are two functionally different types of fat: white adipose tissue (WAT) and brown adipose tissue (BAT). WAT is the primary site of energy storage and also synthesizes and releases a variety of cytokines and hormones that modulate the actions of insulin. Obesity results from excessive accumulation of WAT. In contrast to WAT, BAT is responsible for energy expenditure in the form of thermogenesis. Uncoupling protein-1 (UCP-1) is expressed only in BAT and uncouples oxidative phosphorylation from ATP generation, resulting in the production of heat instead of ATP. BAT deposits are present in all mammals, but in humans these deposits were believed to be nonfunctional except in newborns. However, over the past 4 years it has become evident that BAT has an important role in human adults in the regulation of energy expenditure (Cypess et al., 2009; Nedergaard et al., 2007; Saito et al., 2009; Virtanen et al., 2009; Zingaretti et al., 2009). These studies indicate that BAT activity is inversely correlated with the severity of the metabolic syndrome and that BAT is a major contributor to maintain a lean phenotype. Thus, intervention to increase BAT activity and/or mass is a viable strategy to treat obesity.

Canonical activation of the Jak/Stat pathway involves cytokine and growth factors binding to their cell surface receptors resulting in activation of one or several Jak kinases, which tyrosine phosphorylate specific residues in the cytoplasmic domains of the receptors. Tyrosine phosphorylated receptors provide docking sites for the Stats through their SH2 domains. The activated Jaks also phosphorylate tyrosine on one or several Stats (Raz et al., 1994; Stark et al., 1998). Tyrosine phosphorylated Stats form homodimers or heterodimers, translocate to the nucleus, and bind to regulatory elements in the promoters of cytokine-stimulated early response genes (Decker et al., 1991; Pearse et al., 1991). Activation of the Jak kinase Tyk2 leads to tyrosine phosphorylation of Stat3 in response to different cytokines including type one interferons, IL-12 and IL-23.

Up to now, no evidence existed that Tyk2, a Jak kinase family member, has any role in the pathogenesis of obesity. In this study we make the novel observations that expression of Tyk2 is required for differentiation of Myf5+ brown adipocytes, and that Tyk2-/- mice become obese with age. Furthermore, Tyk2 levels are regulated by diet in mice, and Tyk2 levels are decreased in obese humans. Expression of constitutively active Stat3, (CAStat3) can restore BAT differentiation of Tyk2-/- preadipocytes and reverse the obese phenotype in Tyk2-/- mice. Moreover, rosiglitazone-induced stabilization of PRDM16 protein is absent in Stat3-/- brown preadipocytes under conditions, where there is no change in levels of PRDM16 RNA, suggesting a new mechanism of Stat3 action.The data in this proposal provide new evidence for the unanticipated role of Tyk2 and Stat3 in the regulation of BAT differentiation and energy balance

Results

We observed that Tyk2-/- mice weighed more than their wild type littermates. By 12 months of age the Tyk2-/- animals were approximately 20 grams heavier than Tyk2+/+ mice

(**Fig. 1A**). However, increased weights were observed as early as 12-16 weeks of age on normal chow diet (**Fig. 1B**). Tyk2-/- mice displayed abnormal glucose clearance suggestive of insulin resistance (**Fig. 1C**), as well as many other metabolic abnormalities, including elevated plasma insulin, cholesterol and free fatty acid levels (**Supplemental Table. S1**). Due to different susceptibilities of many mice strains to developing obesity, we examined whether Tyk2-/- mice on C57BL/6 and SV129 backgrounds became obese. Both Tyk2-/- mice on a C57BL/6 and SV129 background showed augmented weights on a normal chow diet. Furthermore, we observed the same metabolic defects in B10.Q/J mice that have a spontaneous mutation in Tyk2 (data not shown) (Shaw et al., 2003). A complete metabolic profile was obtained on 12 week old animals. When normalized to lean body mass (LBM) Tyk2-/- mice showed lower energy expenditure (**Supplemental Fig. S1A and S1B**) and produced 20% less heat (**Supplemental Fig. S1C**) during both, day and night cycles. No changes in food intake (Tyk2+/+ 13.4±5.5 g/48 hrs vs. Tyk2-/- 12.9±2.6 g/48 hrs) or physical activity were detected between Tyk2+/+ and Tyk2-/- mice.

Tyk2 is ubiquitously expressed protein, whose concentrations vary between tissues (Strobl et al., 2011). The protein is abundant in BAT, WAT and spleen and is present in lower amounts in SKM and liver (**Supplemental Fig. S2A**). We examined, whether changes in energy expenditure might control the levels of Tyk2 expression in tissues. C57BL/6 Tyk2+/+ mice were placed on a high fat diet (HFD) for 12 weeks and Tyk2, Jak1 and Jak2 RNAs were analyzed in liver, skeletal muscle (SKM), BAT and WAT. Tyk2 RNA was selectively decreased in BAT and skeletal muscles by approximately 70% in mice on a HFD compared to those on normal chow (**Fig. 1D**), whereas Tyk2 RNA levels in WAT or liver were not changed. The expression of Tyk2 protein was also significantly decreased by 56% ($p<0.05$) in BAT from mice placed on a HFD (**Supplemental Fig. S2B**). Levels of Tyk2 protein in SKM from animals on a HFD were decreased 50% ($p<0.05$). Jak1 and Jak2 RNAs were not altered in mice placed on a HFD (**Supplemental Fig. S2C and S2D**). Similarly to mice fed a HFD, leptin deficient mice (*ob/ob)* also displayed decrease in Tyk2, but not Jak1 or Jak2 RNA in BAT (**Supplemental Fig. S2E**).

We also examined the levels of Tyk2 RNA from rectus abdominus muscle samples obtained from obese humans with or without type II diabetes (T2D). Tyk2 RNA levels were 57% lower in the obese subjects and 52% lower in the obese-diabetic subjects, when compared with lean control subjects (**Fig. 1E**). There was no differences in Jak1 or Jak2 expression between the groups (**Supplemental Fig. S2F**).

Reduced energy expenditure in Tyk2-/- mice suggested additional abnormalities in BAT-specific gene expression in Tyk2-/- mice. Expression of uncoupling protein 1 (UCP1), PRDM16, and Cidea (cell death-inducing DFFA-like effector a) was diminished in BAT isolated from 16 week old Tyk2-/- mice compared with wild type animals (**Fig. 1F**). Additionally, Tyk2-/- mice showed a defect in the expression of β-oxidation enzymes AOX (acyl-CoA oxidase) and LCAD (long chain acyl-CoA dehydrogenase) in BAT (**Supplemental Fig. S1D**). However, RNAs that are normally highly expressed in BAT like PPARγ and PGC1α were not different between Tyk2+/+ and Tyk2-/- animals. The protein levels corresponding to these RNAs were also decreased in BAT of Tyk2-/- mice (**Fig. 1G**). Defects in the morphology of BAT from Tyk2-/- animals were obvious by hematoxylin and eosin staining. Tyk2-/- BAT cells contained large unilocular fat droplets, whereas Tyk2+/+ BAT showed multilocular fat droplets (**Fig. 1H**).

We also examined the mitochondrial morphology of BAT from Tyk2+/+ and Tyk2-/- mice using transmission electron microscopy. The mitochondria of Tyk2-/- BAT and skeletal muscle showed disorganized cristae, but no alterations in mitochondria morphology was observed in the heart (**Supplemental Fig. S3A**).

Mitochondrial function and ultrastructure depend on the proper fusion of the outer and inner membranes (Zick et al., 2009). The fusion processes are governed by three large GTPases: mitofusin 1 (Mfn1), mitofusin 2 (Mfn2) and optic atrophy protein 1 (OPA1). Mfn1 and Mfn2 are involved in early steps of outer membrane fusion, whereas OPA1 is associated with inner membrane fusion and cristae remodeling (Chen and Chan, 2010). Disorganization of mitochondrial cristae observed in BAT and skeletal muscles from Tyk2 deficient mice

correlated with decreased OPA1 expression in these tissues (**Supplemental Fig. S3B**). Reduced mRNA levels of OPA1 were not observed in the control tissues, such as WAT or liver. The expression levels of Mfn1 in SKM and Mfn2 in BAT were modestly changed (**Supplemental Fig. S3C and S3D**). It is notable that elevated expression of these RNAs is associated with an insulin-sensitive phenotype in humans (Lidell et al., 2011). Since BAT and skeletal muscles originate from the same Myf5 positive progenitor cells, (Seale et al., 2008), we conclude that Tyk2 kinase may be important at an early stage of development of these progenitors.

To further confirm a functional defect in Tyk2-/- BAT, oxygen consumption assays were performed using isolated mitochondria from Tyk2+/+ or Tyk2-/- BAT (**Fig. 1I**). Compared with Tyk2+/+ mitochondria, oxygen consumption was decreased in Tyk2-/- mitochondria using pyruvate and malate as substrates for complex I activity and succinate for complex II activity. Addition of GDP, which inhibits the activity of UCP1, decreased O_2 consumption of Tyk2+/+, but not Tyk2-/- mitochondria. The addition of DNP (an uncoupler of OXPHOS) increased O_2 consumption of Tyk2+/+ and Tyk2-/- mitochondria. The respiratory activities of Tyk2-/- mitochondria were comparable to those reported in BAT mitochondria from UCP1 deficient mice (Dlaskova et al., 2010).

Since BAT plays a central role in nonshivering thermogenesis, which maintains body temperature during cold exposure, we examined body temperature and the induction of UCP1 in mice exposed to 4^0C for 12 hrs. There was a significant induction in UCP1 RNA in BAT in Tyk2+/+ but not in Tyk2-/- mice (**Fig.1J**). Body temperatures were also significantly lower in Tyk2-/- animals (**Fig. 1K**). The mechanisms for enhanced sensitivity to cold in Tyk2-/- mice may be due to dysfunctional BAT, which controls nonshivering thermogenesis and/or from a defect in skeletal muscle that is responsible for shivering thermogenesis.

Decrease in BAT-specific RNAs was also observed in *in vitro differentiated* brown preadipocytes isolated from the interscapular BAT of Tyk2-/- mice (**Table 1**). Tyk2-/- preadipocytes did not differentiate as indicated with Oil red O staining (**Fig. 2A**). Furthermore, Tyk2-/- preadipocytes were infected with retroviruses expressing Tyk2, constitutively active Stat3 (CAStat3) or the empty vector (MSCV) and subjected to *in vitro* differentiation (Tseng et al., 2004). Cells expressing Tyk2 or CAStat3, but not the control vector, became Oil red O positive (**Fig. 2A**). Levels of BAT-specific RNAs were completely restored by expressing CAStat3, and were partially restored by Tyk2 (**Table 1**). The explanation as to why the expression of wild type Tyk2 failed to completely restore BAT-specific RNAs is not clear.

Since BAT and skeletal muscle share a common progenitor, and PRDM16 levels are diminished in Tyk2-/- preadipocytes (Seale et al., 2008), we analyzed expression of skeletal muscle-specific genes. The three muscle-selective markers MCK, MyoD and Myg were all elevated in Tyk2-/- compared with Tyk2+/+ preadipocytes (**Table 1 lower panel**). Interestingly, the expression of CAStat3 in Tyk2-/- preadipocytes was much less effective than Tyk2 in decreasing the levels of muscle-specific RNAs (**Table 1**). These results suggest that there are two different functions of Tyk2: one is to induce the expression of BAT-specific genes, which is effectively accomplished by the expression of Tyk2 or CAStat3. The other is the repression of skeletal muscle markers, which requires Tyk2 and is poorly restored by the expression of CAStat3.

UCP1 and Cidea are expressed in BAT and their expression in brown adipocytes is regulated by DNA methylation and chromatin remodeling (Karamanlidis et al., 2007; Karamitri et al., 2009; Shore et al., 2010). Using bisulphite sequencing we determined the methylation status of the CpGs in the promoters of UCP1 and Cidea genes. We observed hypermethylation of DNA within these promoters in Tyk2-/- preadipocytes (**Supplemental Fig. S4A**), especially at the regions containing the C/EBPβ binding sites, which are crucial for the expression of UCP1 and Cidea (**red frames in Supplemental Fig. S4A)**. Furthermore, the abundance of trimethylated histone H3 at lysine 4 (H3K4me3), which is a mark of transcriptionally active chromatin was lower in the UCP1 and Cidea promoters in Tyk2-/- differentiated brown adipocytes (**Supplemental Fig. S4B and S4C**). As an internal control, we examined the abundance of H3K4me3 at the p16 promoter, which was the same in Tyk2+/+ and Tyk2-/- preadipocytes (**Supplemental Fig. S4D**). p16 expression and methylation are not affected by BAT differentiation.

Since CAStat3 rescues differentiation in Tyk2-/- preadipocytes, we examined whether Stat3 was required for brown adipocyte differentiation. Stable preadipocyte lines were created using shRNA directed against Stat3 or a scrambled control (SCR). Western blot analysis showed complete loss of Stat3 protein (**Fig. 2B**), which correlated with decreases in BAT-specific gene expression (UCP1, Cidea) but not in adipogenic markers (PPARγ and aP2) (**Fig. 2C**). The normal levels of PPARγ and aP2 in these cells is consistent with the observation that they display normal adipogenesis and become Oil red O positive (data not shown).

PRDM16 and C/EBPβ control the conversion of myoblastic precursors to brown adipocytes and are sufficient to induce differentiation of fully functional brown adipocytes from nonadipogenic embryonic fibroblasts (Seale et al., 2008; Seale et al., 2007). Since PRDM16 is a master regulator of BAT development, we tested if its over expression could induce differentiation in Tyk2-/- preadipocytes. Tyk2-/- cells were infected with retroviruses expressing PRDM16 and/or C/EBPβ. PRDM16 expression increased the differentiation of brown adipocytes as demonstrated both by Oil red O staining (**Fig. 3A**) and gene expression **(Table 2).** Expression of C/EBPβ alone had no effect on differentiation of Tyk2-/- brown preadipocytes **(Fig. 3A).** However, a combination of both PRDM16 and C/EBPβ fully restored differentiation of Tyk2-/- preadipocytes to the level observed in Tyk2+/+ cells. Furthermore, immunoprecipitation of PRDM16 from these cells demonstrated that endogenous Stat3 formed a complex with PRDM16 **(Fig. 3B).** We have also detected the complex in cell extracts immunoprecipitated with Stat3 **(Fig. 3C)**, as well as in adipocytes, which express endogenous levels of PRDM16 and Stat3 **(Fig. 3D).** We have not observed any changes in the association of PRDM16 and Stat3 in cells treated with rosiglitazone (data not shown).

Treatment of preadipocytes with the PPARγ agonist rosiglitazone stabilizes PRDM16 protein (Ohno et al., 2012). Since PRDM16 intereacts with Stat3 and the expression of both is required for differentiation of brown adipocytes, we examined PRDM16 protein levels in Stat3+/+ and Stat3-/- preadipocytes incubated with or without rosiglitazone, while the cells were being differentiated (**Fig. 3E**). Basal levels of PRDM16 protein were very much decreased or absent in differentiated Stat3-/- adipocytes and rosiglitazone induction of PRDM16 was severely blunted. We also incubated cells with or without rosiglitazone under nondifferentiating conditions (**Fig. 3F**). Although basal levels of PRDM16 were similar in Stat3+/+ and Stat3-/- cells prior to differentiation, rosiglitazone did not increase the expression of PRDM16 in Stat3-/- cells. Furthermore, expression of PPARγ was not altered in Stat3-/- preadipocytes.

In contrast to levels of PRDM16 protein, as reported by Ohno et al, (Ohno et al., 2012), levels of PRDM16 RNA were not significantly changed in Stat3+/+ or Stat3-/- brown adipocytes with or without exposure to rosiglitazone (**Fig. 3G**).

To determine whether the metabolic syndrome in Tyk2-/- mice was due to a defect in BAT development, we examined a mouse containing a constitutively active Stat3 transgene, whose expression is activated by Cre recombinase (Mesaros and Barsh, 2008). CAStat3 mice were crossed with Tyk2-/- mice (Tyk2-/-CAStat3). Tyk2-/-CAStat3 mice were then crossed with aP2 Cre/Tyk2-/- mice that express Cre recombinase in adipose tissue to generate aP2-Cre/Tyk2-/-CAStat3 mice (Imai et al., 2001). Consistent with the results of Mesaros et al (Mesaros and Barsh, 2008) the transgene was expressed at physiological levels (data not shown). All experiments were performed using Tyk2-/- CAStat3 (controls-CTR) and animals with the activated transgene aP2-Cre/Tyk2-/-CAStat3 (CAStat3), from the same litter. As previously reported, transgenes expressed under the control of the aP2 promoter can be variably expressed in BAT, WAT or both tissues (Cho et al., 2009). Expression of the CAStat3 transgene preferentially in BAT of Tyk2-/- mice upregulated the levels of BAT-specific RNAs (UCP1, PRDM16, Cidea), which are severely diminished in Tyk2-/- animals (**Fig. 4A**). C/EBPβ, PPARγ and PPARα, which play important roles in BAT development, were also increased. The protein levels corresponding to these RNAs were also increased in BAT of CAStat3 mice (**Fig. 4B**). Furthermore, the altered BAT morphology depicted in (**Fig. 1H)** was restored by CAStat3 expression and resembled the tissue in wild type animals (**Fig. 4C**). Tyk2-/- mice expressing CAStat3 in BAT exhibited significantly

reduced body weight in comparison to control littermates (**Fig. 4D**). Moreover, CAStat3 mice had much lower plasma insulin levels than control animals, suggesting improved insulin sensitivity (**Fig. 4E**). The levels of insulin as well as body weight in the transgeneic mice were similar to wild type animals (data not shown).

Discussion:

The data in this report provide new evidence for the unanticipated role of Tyk2 and Stat3 in the regulation of Myf5+ BAT development and energy balance both in rodents and possibly humans. Tyk2-/- mice provide a new model to understand the role of BAT in pathogenesis of obesity. The observations that Tyk2 RNA in BAT and skeletal muscle is regulated by diet in rodents, and obese humans, who also have decreased levels of Tyk2 in skeletal muscle, offers new potential avenues for pharmacological and nutritional intervention to treat obesity*.*

At the moment it is not clear whether the obese phenotype observed in Tyk2-/- mice is only due to impaired differentiation of BAT or whether a defect in SKM also contributes to obesity. Since we have used global Tyk2 knock out animals for these studies, it is also possible that the changes in overall metabolism are a result of a multiple defects in more than one tissue. The fact that the CAStat3 transgene expressed in BAT of Tyk2-/- mice restores a normal phenotype argues that the actions of Stat3 do not required its activation in SKM. These results also argue against the concept that a defect in many tissues in the Tyk2-/- mouse is required for the development of obesity. It remains to be determined, whether the actions of Tyk2 are mediated through Stat3 and/or another signaling pathway.

White and brown adipocytes are derived from mesenchymal stem cells. Interscapular BAT shares a common lineage with Myf5+ muscle progenitors, while brown adipocyte-like cells distributed within subcutaneous WAT and skeletal muscle have a different lineage (Schulz et al., 2011). Recent studies indicate that this model is more complex in that mixtures of Myf5+ and Myf5- cells are present in WAT (Sanchez-Gurmaches et al., 2012). Differentiation of Myf5+ progenitors into brown preadipocytes requires the expression of PRDM16. Our results suggest that Tyk2 and Stat3 are required for the progression of differentiation-incompetent preadipocytes to committed differentiation-competent brown preadipocytes such that PRDM16, C/EBPβ, Stat3, and other TFs can induce differentiation. It remains to be determined, whether Tyk2 and Stat3 directly or indirectly mediate the expression of BAT-selective RNAs. The fact that the DNA in the promoters of UCP1 and Cidea are hypermethylated in Tyk2-/- preadipocytes and markers of the abundance of trimethylated histone H3 at lysine 4 (H3K4me3) are decreased is consistent with an effect of Tyk2 on chromatin modeling.

This leads us to speculate that the role of Tyk2 in differentiation of BAT is to directly or indirectly facilitate chromatin remodeling and accessability. A nuclear-localized pool of the related kinase Jak2 phosphorylates histone H3 (Dawson M.A., 2010). It is notable that Tyk2 also localizes to the nucleus (Ragimbeau et al., 2001). It is thus possible that the actions of Tyk2 are unrelated to those of Stat3 and classic cytokine activation of the Jak/Stat pathway. An alternative or additional role of Tyk2 might be to modify Stat3 such that in combination with PRDM16 and C/EBPβ it induces the expression of BAT-specific genes. Under this scenario, CAStat3 would be modified in the absence of Tyk2 such that it can induce differentiation of Tyk2-/- preadipocytes. Tyrosine phosphorylation of Stat3 probably is not the modification of this protein mediated by Tyk2 because both basal levels of tyrosine phosphorylated Stat3 in preadipocytes, and tyrosine phosphorylated Stat3 during differentiation are not different between Tyk2-/- and Tyk2+/+ cells (data not shown). Acetylation and methylation have been reported to modify Stat3 and contribute to the effects of Stat3 in gluconeogenesis (Nie et al., 2009; Yang et al., 2010).

In contrast to the ability of CAStat3 to induce BAT-specific gene expression, CAStat3 does not substitute for wild type Tyk2 in repressing the expression of muscle specific genes during differentiation of preadipocytes (**Table 1**). Disrupted expression of Stat3 in Tyk2+/+ preadipocytes diminished BAT-selective gene expression, indicates that this transcription factor plays an essential role in two stages of BAT development: the progression of

differentiation-incompetent to differentiation-competent preadipocytes, and the development of differentiation-competent adipocytes into mature brown adipocytes. At the moment it is not clear whether progression from differentiation-competent to mature brown adipocytes requires Tyk2.

The expression of CAStat3 in BAT of Tyk2-/- mice is consistent with the results in cell culture models. However, the aP2 Cre promoter used to express CAStat3 in Tyk2-/- mice is also expressed in macrophages and brain, leaving the possibility that these tissues may also be involved in the obese phenotype (Kloting et al., 2008; Mao et al., 1993; Urs et al., 2006). We have not detected expression of CAStat3 in macrophages indicating that they do not contribute to the actions of CAStat3 in preventing the development of obesity. We have not examined, whether CAStat3 mice express the transgene in brain. However, if CAStat3 expression in the brain is contributing to the prevention of obesity, then we would expect to see changes in the metabolic profile of mice that express CAStat3 only in WAT and brain. The limited numbers of animals that express CAStat3 only in WAT that have been examined, display the same phenotype as Tyk2-/- mice. These results suggest that it is unlikely that expression of CAStat3 in the brain is contributing to the obesity observed in Tyk2-/- mice.

The observation that rosiglitazone-induced stabilization of PRDM16 protein is absent in Stat3-/- brown preadipocytes under conditions, where there is no change in levels of PRDM16 RNA suggests a new mechanism of Stat3 action. We have examined whether the expression of Stat3 controls the rate of degradation of PRDM16 by treating cells with cycloheximide (Ohno et al., 2012). There were no changes in half life of PRDM16 protein in Stat3-/- compared to Stat3+/+ preadipocytes, suggesting that in these cells the rate of translation of PRDM16 is being influenced by the presence of Stat3. However, these results are ambiguous because the endogenous levels of PRDM16 are very low in Stat3-/- cells which makes it very difficult to analyze rates of decay of the protein. Stat3 may directly stabilize PRDM16 protein, presumably by their direct interaction (**Fig. 3B, 3C and 3D**). Alternatively, Stat3 may regulate the expression of RNAs that encode proteins involved in stability of PRDM16. Since PRDM16 is destabilized through the ubiquitin (Ub)-proteasome targeting system, this complex is also a potential target of Stat3. In renal cancer cells Stat3 has been reported to bind and stabilize HIF1a but the physiological consequences of this interaction need to be clarified (Jung et al., 2005).

Further characterization of the mechanisms by which Tyk2 and Stat3 regulate brown fat development in animal models and a better understanding of the signaling cascade governed by these proteins will help design screens for new targets to treat obesity and the metabolic syndrome.

Materials and methods:

Reagents and antibodies

All chemicals and reagents were purchased from Sigma-Aldrich or indicated otherwise. For western blot analysis, antibodies were purchased from Cell Signaling (mouse monoclonal Stat3 and rabbit polyclonal PPARγ), Sigma-Aldrich (mouse monoclonal alpha-tubulin), Abcam (rabbit polyclonal PPARα and rabbit polyclonal UCP1), Life Span Biosciences (rabbit polyclonal Cidea). Tyk2 antisera were a kind gift of Dr. Birgit Strobl (University of Veterinary Medicine, Vienna, Austria). PRDM16-specific rabbit polyclonal antibodies were a kind gift of Dr. Patrick Seale (University of Pennsylvania, School of Medicine, Philadelphia, USA).

Subjects

Ten lean controls (4 men, 6 women; average age: 45.3 ± 2.8), 15 obese (3 men, 12 women; average age: 36 ± 2.1) and 12 obese type-2 diabetic (8 men, 4 women; average age: 49.3 ± 1.4) individuals participated in this study. Obese and obese type-2 diabetic patients were undergoing laparoscopically performed adjustable gastric banding surgery, as previously described (O'Brien et al., 2005). None of the patients were under thiazolidinedione but some of them under insulin treatment. Lean patients were undergoing general abdominal surgical procedures unrelated to obesity or type-2 diabetes. The subject details have been published previously (Russell et al., 2012). Written informed consent was obtained from all subjects. This study was approved by the Deakin University Human Ethics Research Committee, The Avenue Hospital and Cabrini Hospital. Muscle samples (about 200 mg) were obtained from the rectus abdominus in the fasted state (8-18 hrs). All participants were under general anaesthesia, predominantly via short-acting propofol and maintained by a fentanyl, rocuronium and volatile anaesthesia mixture. Following collection, which was performed 30 min after the operation had started, surgical samples were immediately frozen in liquid nitrogen.
Statistical analysis was performed using SPSS version 15.0. A one-way analysis of variance (ANOVA) followed by LSD or Dunnett's T3 *post-hoc* test was used (where equal variances were not assumed) to determine the significance of differences between groups. Significance was set at $p<0.05$.

Animals

All the mice were bred and maintained in the MCV/VCU animal facility according to Institutional Animal Care and Use Committee (IACUC) regulations. Male mice were used for these studies. Tyk2 deficient mice (C57BL/6) were kindly provided by Dr. Ana Gamero (Temple University School of Medicine, Philadelphia, USA). Tyk2-/- (SV129) were generated by Dr. Kazuya Shimoda and colleagues (Kyushu University, Fukuoka, Japan) (Shimoda et al., 2000). Mice carrying a transgene encoding a constitutively active form of the Stat3 protein (CAStat3) including an upstream loxP- flanked stop sequence in the ubiquitously expressed Rosa26 locus were a kind gift of Dr. Klaus Rajewsky (Harvard Medical School, Boston, USA) (Mesaros and Barsh, 2008) . The Tyk2-/- mice expressing the constitutively active Stat3 only in BAT (brown adipose tissue) or WAT (white adipose tissue) were obtained by crossing CAStat3 transgenic animals with mice expressing the Cre recombinase under control of the aP2 promoter, allowing adipocyte-specific expression of Cre. Both transgenic lines (CAStat3 and aP2-Cre) were bred with Tyk2-/- mice and then intercrossed. Only animals from the same mixed background strain generation were compared. The specificity of transgene expression was confirmed by qPCR. Mice carrying floxed alleles of Stat3 were kindly provided by Dr. Valeria Poli (University of Turin, Italy).

Cell Culture

Interscapular brown adipose tissue was isolated from newborn Tyk2+/+ and Tyk2-/- mice, minced and subjected to collagenase A digestion (1.5 mg/ml in isolation buffer containing 123 mM NaCl, 5 mM KCl, 1.3 mM $CaCl_2$, 5 mM glucose, 100 mM HEPES and 4% BSA) for 40 min at 37^{o}C (Fasshauer et al., 2000). Collected cells were centrifuged at 1500 rpm at room temperature for 5 min and then resuspended in 1 ml of primary culture medium (Dulbecco's modified Eagle medium, 4500 mg/L glucose Gibco, Carlsbad, CA) containing 20% FBS, 20 mM HEPES and 1% penicillin-streptomycin), transferred into 12 well plates and grown in a humidified atmosphere of 5% CO_2 and 95% O_2 at 37°C. After 3 days of culture, cells were immortalized by infection with puromycin resistance retroviral vector pBabe encoding SV40 Large T antigen. 24 hrs after infection cells were split into 10 cm dishes and maintained in primary culture media for the next 24 hrs and then subjected to selection with puromycin at a concentration of 2 µg/ml in DMEM with 20% FBS for one week.
For differentiation, brown preadipocytes were grown to 100% confluence in the differentiation medium: DMEM containing 4500 mg/L glucose, 10% FBS, 20 nM insulin and 1 nM triiodothyronine. Fully confluent cells were incubated for 48 h in differentiation medium supplemented with 0.5 mM isobutylmethylxanthine (IMBX), 0.5 µM dexamethasone and 0.125 mM indomethacin (induction medium). After 48 hrs of induction, cells were maintained in differentiation medium for 5 days.

Constructs and viral transductions

293T cells, used as packaging cells, were grown in complete DMEM medium containing 10% FBS and 1% penicillin-streptomycin. Cells were transfected in 10 cm dishes using Fugene reagent (Roche Diagnostics, Indianapolis, IN) according to the manufacturer's instructions. The virus-containing medium was collected 48 hrs after transfection, centrifuged for 10 min at 500 x g and filtered through 0.45 µm filter. Viral supernatants were added to the cells for 12 hrs in the presence of Polybrene (8 µg/ml polybrene, Chemicon Int., Temecula,CA), then diluted twice with the fresh medium. The next day the viral supernatant was removed and replaced by fresh medium.
Retroviral vectors to express Tyk2, CAStat3, PRDM16 and C/EBPβ have been previously described (Potla et al., 2006)**.** Lentiviral vector expressing shRNA targeting Stat3 (pFLRu-shtat3-YFP) and helper vectors (CMV-VSV-G and pHR'8.2deltaR) were a kind gift of Dr. Barry Sleckman (Washington University, School of Medicine, St. Louis, USA). Retroviral vector expressing Cre recombinase was kindly provided by Dr. Michael David (University of California, San Diego, USA).

Dietary studies

Five week old mice were housed four or five per cage and maintained on a fixed 12 hrs light/dark cycle. The animals were fed regular chow diet (Teklad F6 S664, Harlan Tekland, Madison, WT) or high-fat diet (D12330, Research Diets, New Brunswick, NJ). The chow diet contained 27% kcal protein, 17% kcal fat and 57% kcal carbohydrate. The high-fat diet contained 20% kcal protein, 60% kcal fat and 20% kcal carbohydrate. The mice were kept on the diets for 12 weeks. They had free access to water and food.

Glucose tolerance test (GTT)

Mice were fasted overnight (16 hrs) and then 2 mg/g glucose was injected intraperitoneally. Blood glucose levels were measured using a One-Touch Ultra glucometer (LifeScan, Milpitas, CA) at 0, 15, 30, 60 and 120 min after glucose administration.

Biochemical analysis

Mice were fasted overnight (16 hrs). Blood samples were collected performing heart punctures. Plasma samples were obtained by centrifuging blood in Microtainer plasma separator tubes (Becton Dickinson, Frankiln Lakes, NJ). Plasma was assayed for insulin using an Ultra sensitive mouse insulin ELISA kit (Crystal Chem Inc, Downers Grove, IL). The measurements of blood cholesterol, β-hydroxybutyrate, FFA and triglycerides were performed by the Cincinnati Mouse Metabolic Phenotyping Center (MMPC).

Mitochondrial preparation

Brown adipose tissue mitochondria were prepared as described previously (Shabalina et al., 2004). Briefly, four Tyk2+/+ and/or Tyk2-/- mice were sacrificed for each experiment. The interscapular brown adipose tissue depots were dissected out, cleaned from white adipose tissue and pooled in ice-cold isolation buffer (250 mM sucrose, 10 mM Tris-HCl, 1mM EDTA, 0.2% defatted BSA). The tissue was kept at 4°C throughout the isolation process. The tissue was minced with scissors, homogenized in a glass homogenizer with Teflon pestle and centrifuged 8500 x g for 10 min. The supernatant containing fat layer was discarded. The pellet was resuspended in isolation buffer and centrifuged at 500 x g for 10 min. The resulting supernatant was transferred to a clean tube and centrifuged again at 8500 x g for 10 min. The mitochondrial pellet was resuspended in KME buffer pH 7.4 (100 mM KCl, 50 mM MOPS, 0.5 mM EGTA) and used within 4 hrs after isolation. The protein concentration was measured using the Lowry method (with BSA as a standard and sodium deoxycholate as a detergent) (Lowry et al., 1951).

Oxygen consumption

Oxygen consumption was measured using a Clark-type oxygen electrode (Strathkelvin Instruments, North Lanarkshire, UK) at 30 °C in respiration buffer at pH 7.4 (100 mM KCl, 50 mM MOPS, 1 mM EGTA, 5 mM KH_2PO_4, 0.1% defatted BSA). The mitochondrial suspension was continuously stirred in the chambers using magnetic stirrers. Oxygen consumption rates were measures in the presence of the substrate of interest: for complex I (5 mM pyruvate plus 5 mM malate), for complex II (20 mM succinate with 7.5 μM rotenone). Subsequently, 1 mM GDP and 0.2 mM dinitrophenol (DNP) were added.

Measurement of energy expenditure by indirect calorimetry

Metabolic rates were measured by indirect calorimetry in Tyk2+/+ and Tyk2-/- mice by using an 8-chamber open-circuit Oxymax system (CLAMS, Columbus Instruments,Columbus, OH) at Mouse Metabolic Phenotyping Center in the Case Western Reserve University (Cleveland, Ohio). Briefly, mice were individually housed in acrylic calorimeter chambers through which air of known O_2 concentration was passed at a constant flow rate. The system automatically withdrew gas samples from each chamber hourly for 24 h. The system then calculated the volume of O_2 consumed (VO_2) and CO_2 generated (VCO_2) for each mouse in 1 h normalized by lean body mass. Body composition of unanesthetized mice was measured by quantitative magnetic resonance imaging using EchoMRI (Echo Medical Systems, Houston, TX) as previously described (Lo et al., 2008). The RQ, ratio of the VCO_2 to VO_2, was calculated. Heat expenditures were measured throughout the study in light and dark cycles and under fed and fasting conditions and represented in kcal/g/day. Mice were maintained at 25°C and had free access to water under all conditions.

Histology

Brown adipose tissues were fixed in 10% formalin and were paraffin-embedded. Multiple sections were prepared and stained with hematoxylin and eosin (H&E) at the Pathology Research Service Facility (VCU Medical Center, Richmond, VA).

Electron microscopy

Brown adipose tissue, skeletal muscle and heart were fixed in 2% paraformaldehyde- 2% glutaraldehyde in 0.1 M cacodylate buffer. The tissue samples were processed and analyzed at the Microscopy Core Facility at the Department of Anatomy and Neurobiology (VCU Medical Center, Richmond, VA).

Oil red O staining

The Oil red O staining protocol was used to test for lipid accumulation in fully differentiated cells. Plates with cells were rinsed once with PBS and then fixed with buffered formalin for 1 hr at room temperature. Fresh Oil red O working solution was prepared by adding 6 ml of the stock solution (0.5 g Oil red O in 100 ml of 2-propanol) to 4 ml of dH_2O, mixed and filtered through Whatman filter paper. Following fixation the cells were incubated for 1hr at room temperature with Oil red O stain. Then plates were carefully rinsed several times with dH_2O and air-dried before collecting images under the inverted microscope.

RNA extraction and real-time qPCR

Total RNA was isolated with TRI Reagent (Molecular Research, Cincinnati, OH), according to the manufacturer's instructions. Isolated RNA samples were treated with DNase (Promega, Madison, WI), cDNA was synthesized from 2 µg of RNA with the Tetro cDNA Synthesis Kit (Bioline, Taunton, MA), real-time qPCR was performed using SensiMix SYBR and Fluorescein Kit (Bioline, Taunton, MA) according to manufacturer's instruction. All the samples were assayed in duplicates and analyzed using a CFX96 Real-Time PCR Detection System (Bio-Rad, Hercules, CA). **Table S2** contains a full list of the primer sequences. Primer for Tyk2, Jak1, Jak2, OPA1, Mfn1 and Mfn2 were purchased from SuperArray (Qiagen SABioscience, Frederick, MD).

Western blot analysis

Cells / tissues were lysed in ice-cold extraction buffer (20 mM HEPES, 300 mM NaCl, 10 mM KCl, 1 mM $MgCl_2$**,** 20% glycerol, 1% Triton X-100) with added protease and phosphatase inhibitor cocktails (Roche, Indianapolis, IN) for 30 min at 4°C. After lysis, cell debris was removed from the lysates by centrifugation at 20,000 x g for 20 min at 4°C. The protein concentration in the supernatants was determined using a Bio-Rad protein assay (Bio-Rad, Hercules, CA). Equal amounts of protein were mixed 1:1 with 2X Laemmli sample buffer containing 1 mM β-mercaptoethanol, separated using SDS-PAGE electrophoresis and transferred to Immobilon-P PVDF membranes. Membranes were blocked for 1 h at room temperature with 5% non-fat dry milk and then incubated overnight at 4^oC with the indicated primary antibodies. Amersham ECL Plus Western Blotting Detection Reagent (GE Healthcare Life Sciences, Piscataway, NJ) was used for chemiluminescent detection. Image J software was used for quantifying the intensity of signals.

Immunoprecipitation

Whole cell extracts were incubated overnight at 4°C with PRDM16 antibodies or Stat3 rabbit antisera plus agarose beads or control IgG plus agarose beads in an IP buffer pH 7.4 (150

mM NaCl, 50mM Tris-HCl, 1% Triton, 1 mM EDTA with added protease and phosphatase inhibitor cocktails (Roche, Indianapolis, IN). Immunoprecipitates were washed five times with wash buffer (150 mM NaCl, 50mM Tris-HCl, 1% Triton, protease and phosphatase inhibitor cocktails), separated by SDS-PAGE and blotted with indicated antibodies.

Bisulfite sequencing

1.5 µg of genomic DNA was converted using EZ DNA methylation kit (Zymo Research, Orange, CA) according to the supplier's instructions. The treated DNA was amplified by PCR using the bisulfite-specific primers listed in **Table S3**. The amplification conditions for the 830 bp (Cidea promoter) and 730 bp (UCP1 promoter) DNA fragments were as follow: stage 1: 95 ^{o}C/ 3 min/ 1 cycle; stage 2: 95 ^{o}C/ 1 min/ 55 ^{o}C/ 1 min/ 73 ^{o}C/ 1 min/ 40 cycles; stage 3: 73 ^{o}C/ 5 min/ 1 cycle. PCR products were cloned into the pCR2.1-TOPO vector (Invitrogen, Carlsbad, CA), and 8-15 clones for each were picked and sequenced.

Chromatin immunoprecipitation (ChIP) assay.

Immortalized Tyk2+/+ and Tyk2-/- differentiated adipocytes were crosslinked with 1% formaldehyde for 10 min at 37^{o}C and then washed with ice-cold PBS containing 125 mM glycine and 1 mM PMSF. Chromatin was sonicated and immunoprecipitated using specific antibodies exactly as described in the ChIP protocol provided by Upstate Inc. (Charlottesville, VA). The following antibodies were used: ChIPAb+ Trimethyl-Histone H3 (Lys4) from Milipore. The primers used in qPCR are listed in **Table S4**.

Statistical analysis

Results are presented as the mean ± SE. Statistical comparison was performed using two-tailed Student's t-test. While interpreting the data results a p-value less than 0.05 was considered statistically significant and annotated by *.

Acknowledgements

This work was supported in part by R01 AI059710-01 and R21 AI088487 to ACL. BS was supported by the Austrian Science Fund (FWF SFB-F28). We would like to thank Dr. Bruce Spiegelman for his advice.

Correspondence and requests for materials should be addressed to Andrew Larner, Dept. of Biochemistry and Molecular Biology, VCU School of Medicine, MMRB, Rm 2050, 1220 East Broad St. Richmond, VA 23298 Email: (alarner@vcu.ed)

References

Chen, H., and Chan, D.C. (2010). Physiological functions of mitochondrial fusion. Ann N Y Acad Sci 1201, 21-25.

Cho, Y.-W., Hong, S., Jin, Q., Wang, L., Lee, J.-E., Gavrilova, O., and Ge, K. (2009). Histone Methylation Regulator PTIP Is Required
for PPARg and C/EBPa Expression and Adipogenesis. Cell Metabolism 10, 27-39.

Cypess, A.M., Lehman, S., Williams, G., Tal, I., Rodman, D., Goldfine, A.B., Kuo, F.C., Palmer, E.L., Tseng, Y.H., Doria, A., Kolodny, G.M., and Kahn, C.R. (2009). Identification and importance of brown adipose tissue in adult humans. N Engl J Med 360, 1509-1517.

Dawson M.A., B., A. J., Go¨ttgens, B., Foster, S. D., Bartke, T. Green, A. R., Kouzarides, T. (2010). JAK2 phosphorylates histone H3Y41 and excludes
HP1a from chromatin. Nature 461, 819-824.

Decker, T., Lew, D.J., and Darnell, J.E.J. (1991). Two Distinct Alpha-Interferon-Dependent Signal Transduction Pathways May Contribute to Activation of Transcription of the Guanylate-Binding Protein Gene. Mol. Cell. Biol. 11, 5147-5153.

Dlaskova, A., Clarke, K.J., and Porter, R.K. (2010). The role of UCP 1 in production of reactive oxygen species by mitochondria isolated from brown adipose tissue. BBA 1797, 1470-1476.

Fasshauer, M., Klein, J., Ueki, K., Kriauciunas, K.M., Benito, M., White, M.F., and Kahn, C.R. (2000). Essential role of insulin receptor substrate-2 in insulin stimulation of Glut4 translocation and glucose uptake in brown adipocytes. J Biol Chem 275, 25494-25501.

Griffiths, D.S., Li, J., Dawson, M.A., Trotter, M.W., Cheng, Y.H., Smith, A.M., Mansfield, W., Liu, P., Kouzarides, T., Nichols, J., Bannister, A.J., Green, A.R., and Gottgens, B. (2011). LIF-independent JAK signalling to chromatin in embryonic stem cells uncovered from an adult stem cell disease. Nat Cell Biol 13, 13-21.

Imai, T., Jiang, M., Chambon, P., and Metzger, D. (2001). Impaired adipogenesis and lipolysis in the mouse upon selective ablation of the retinoid X receptor alpha mediated by a tamoxifen-inducible chimeric Cre recombinase (Cre-ERT2) in adipocytes. Proc Natl Acad Sci U S A 98, 224-228.

Jung, J.E., Lee, H.G., Cho, I.H., Chung, D.H., Yoon, S.H., Yang, Y.M., Lee, J.W., Choi, S., Park, J.W., Ye, S.K., and Chung, M.H. (2005). STAT3 is a potential modulator of HIF-1-mediated VEGF expression in human renal carcinoma cells. Faseb J 19, 1296-1298.

Karamanlidis, G., Karamitri, A., Docherty, K., Hazlerigg, D.G., and Lomax, M.A. (2007). C/EBPbeta reprograms white 3T3-L1 preadipocytes to a Brown adipocyte pattern of gene expression. J Biol Chem 282, 24660-24669.

Karamitri, A., Shore, A.M., Docherty, K., Speakman, J.R., and Lomax, M.A. (2009). Combinatorial transcription factor regulation of the cyclic AMP-response element on the Pgc-1alpha promoter in white 3T3-L1 and brown HIB-1B preadipocytes. J Biol Chem 284, 20738-20752.

Kloting, N., Koch, L., Wunderlich, T., Kern, M., Ruschke, K., Krone, W., Bruning, J.C., and Bluher, M. (2008). Autocrine IGF-1 action in adipocytes controls systemic IGF-1 concentrations and growth. Diabetes 57, 2074-2082.

Lidell, M.E., Seifert, E.L., Westergren, R., Heglind, M., Gowing, A., Sukonina, V., Arani, Z., Itkonen, P., Wallin, S., Westberg, F., Fernandez-Rodriguez, J., Laakso, M., Nilsson, T., Peng, X.R., Harper, M.E., and Enerback, S. (2011). The adipocyte-expressed forkhead transcription factor Foxc2 regulates metabolism through altered mitochondrial function. Diabetes 60, 427-435.

Lo, C.M., Samuelson, L.C., Chambers, J.B., King, A., Heiman, J., Jandacek, R.J., Sakai, R.R., Benoit, S.C., Raybould, H.E., Woods, S.C., and Tso, P. (2008). Characterization of mice lacking the gene for cholecystokinin. Am J Physiol Regul Integr Comp Physiol 294, R803-810.

Lowry, O.H., Rosebrough, N.J., Farr, A.L., and Randall, R.J. (1951). Protein measurement with the Folin phenol reagent. J Biol Chem 193, 265-275.

Mao, C., Davies, D., Ker, I.M., and Stark, G.R. (1993). Mutant human cell lines defective in induction of major histocompatibility complex class II genes by interferon γ. Proc. Natl. Acad. Sci. U.S.A. 90, 2880-2884.
Mesaros, A., Koralov, S., Rother, E., Wunderlich, F. T., Ernst, M. B., , and Barsh, G.S., Rajewsky, K. and Bruning, J. C. (2008). Activation of Stat3 Signaling in AgRP Neurons Promotes Locomotor Activity Cell Metabolism 7, 236-248.
Nedergaard, J., Bengtsson, T., and Cannon, B. (2007). Unexpected evidence for active brown adipose tissue in adult humans. Am J Physiol Endocrinol Metab 293, E444-452.
Nie, Y., Erion, D.M., Yuan, Z., Dietrich, M., Shulman, G.I., Horvath, T.L., and Gao, Q. (2009). STAT3 inhibition of gluconeogenesis is downregulated by SirT1. Nat Cell Biol 11, 492-500.
O'Brien, P.E., Dixon, J.B., Laurie, C., and Anderson, M. (2005). A prospective randomized trial of placement of the laparoscopic adjustable gastric band: comparison of the perigastric and pars flaccida pathways. Obes Surg. 15, 820-826.
Ohno, H., Shinoda, K., Spiegelman, B.M., and Kajimura, S. (2012). PPARgamma agonists induce a white-to-brown fat conversion through stabilization of PRDM16 protein. Cell Metab 15, 395-404.
Pearse, R.N., Feinman, R., and Ravetch, J.V. (1991). Characterization of the promoter of the human gene encoding the high-affinity IgG receptor: Transcriptional induction by γ interferon is mediated through common DNA response elements. Proc. Natl. Acad. Sci. USA 88, 11305-11309.
Potla, R., Koeck, T., Wegrzyn, J., Cherukuri, S., Shimoda, K., Baker, D.P., Wolfman, J., Planchon, S.M., Esposito, C., Hoit, B., Dulak, J., Wolfman, A., Stuehr, D., and Larner, A.C. (2006). Tyk2 tyrosine kinase expression is required for the maintenance of mitochondrial respiration in primary pro-B lymphocytes. Mol Cell Biol 26, 8562-8571.
Ragimbeau, J., Dondi, E., Vasserot, A., Romero, P., Uze, G., and Pellegrini, S. (2001). The receptor interaction region of Tyk2 contains a motif required for its nuclear localization. J. Biol. Chem. 276, 30812-30818.
Raz, R., Durbin, J.E., and Levy, D.E. (1994). Acute Phase Response Factor and Additional Members of the Interferon-stimulated Gene Factor 3 Family Integrate Diverse Signals from Cytokines, Interferons, and Growth Factors. J. Biol. Chem. 269, 24391-24395.
Russell, A.P., Crisan, M., Leger, B., Corselli, M., McAinch, A.J., O'Brien, P.E., Cameron-Smith, D., Peault, B., Casteilla, L., and Giacobino, J.P. (2012). Brown adipocyte progenitor population is modified in obese and diabetic skeletal muscle. . International journal of obesity 36, 155-158.
Saito, M., Okamatsu-Ogura, Y., Matsushita, M., Watanabe, K., Yoneshiro, T., Nio-Kobayashi, J., Iwanaga, T., Miyagawa, M., Kameya, T., Nakada, K., Kawai, Y., and Tsujisaki, M. (2009). High incidence of metabolically active brown adipose tissue in healthy adult humans: effects of cold exposure and adiposity. Diabetes 58, 1526-1531.
Sanchez-Gurmaches, J., Hung, C.M., Sparks, C.A., Tang, Y., Li, H., and Guertin, D.A. (2012). PTEN Loss in the Myf5 Lineage Redistributes Body Fat and Reveals Subsets of White Adipocytes that Arise from Myf5 Precursors. Cell Metab 16, 348-362.
Schulz, T.J., Huang, T.L., Tran, T.T., Zhang, H., Townsend, K.L., Shadrach, J.L., Cerletti, M., McDougall, L.E., Giorgadze, N., Tchkonia, T., Schrier, D., Falb, D., Kirkland, J.L., Wagers, A.J., and Tseng, Y.H. (2011). Identification of inducible brown adipocyte progenitors residing in skeletal muscle and white fat. Proc Natl Acad Sci U S A 108, 143-148.
Seale, P., Bjork, B., Yang, W., Kajimura, S., Chin, S., Kuang, S., Scime, A., Devarakonda, S., Conroe, H.M., Erdjument-Bromage, H., Tempst, P., Rudnicki, M.A., Beier, D.R., and Spiegelman, B.M. (2008). PRDM16 controls a brown fat/skeletal muscle switch. Nature 454, 961-967.
Seale, P., Kajimura, S., Yang, W., Chin, S., Rohas, L.M., Uldry, M., Tavernier, G., Langin, D., and Spiegelman, B.M. (2007). Transcriptional control of brown fat determination by PRDM16. Cell Metab 6, 38-54.
Shabalina, I.G., Jacobsson, A., Cannon, B., and Nedergaard, J. (2004). Native UCP1 displays simple competitive kinetics between the regulators purine nucleotides and fatty acids. J Biol Chem 279, 38236-38248.

Shaw, M.H., Boyartchuk, V., Wong, S., Karaghiosoff, M., Ragimbeau, J., Pellegrini, S., Muller, M., W.F., D., and Yap, G.S. (2003). A natural mutation in the Tyk2 pseudokinase domain underlies altered susceptibility of B10.Q/J mice to infection and autoimmunity. Proc. Natl. Acad. Sci. U.S.A. 100, 11594-11599.
Shimoda, K., Kato, K., Aoki, K., Matsuda, T., Miyamoto, A., Shibamori, M., Yamashita, M., Numata, A., Takase, K., Kobayashi, S., Shibata, S., Asana, Y., Gondo, H., Sekiguchi, K., Nakayama, K., Nakayama, T., Okamura, T., Okamura, S., Niho, Y., and Nakayama, K. (2000). Tyk2 Plays a Restricted Role in IFNα Signaling, Although It Is Required for IL-12-Mediated T Cell Function. Immunity 13, 561-571.
Shore, A., Karamitri, A., Kemp, P., Speakman, J.R., and Lomax, M.A. (2010). Role of Ucp1 enhancer methylation and chromatin remodelling in the control of Ucp1 expression in murine adipose tissue. Diabetologia 53, 1164-1173.
Stark, G.R., Kerr, I.M., Williams, B.R.G., Silverman, R.H., and Schreiber, R.D. (1998). How Cells Respond to Interferons. Ann Rev. Biochem. 67, 227.
Strobl, B., Stoiber, D., Sex, V., and Mueller, M. (2011). Tyrosine kinase 2 (TYK2) in cytokine signalling and host immunity. Frontiers in Bioscience 16, 3224.
Tseng, Y.H., Kriauciunas, K.M., Kokkotou, E., and Kahn, C.R. (2004). Differential roles of insulin receptor substrates in brown adipocyte differentiation. Mol Cell Biol 24, 1918-1929.
Urs, S., Harrington, A., Liaw, L., and Small, D. (2006). Selective expression of an aP2/Fatty Acid Binding Protein 4-Cre transgene in non-adipogenic tissues during embryonic development. Transgenic Res 15, 647-653.
Virtanen, K.A., Lidell, M.E., Orava, J., Heglind, M., Westergren, R., Niemi, T., Taittonen, M., Laine, J., Savisto, N.J., Enerback, S., and Nuutila, P. (2009). Functional brown adipose tissue in healthy adults. N Engl J Med 360, 1518-1525.
Yang, J., Huang, J., Dasgupta, M., Sears, N., Miyagi, M., Wang, B., Chance, M.R., Chen, X., Du, Y., Wang, Y., An, L., Wang, Q., Lu, T., Zhang, X., Wang, Z., and Stark, G.R. (2010). Reversible methylation of promoter-bound STAT3 by histone-modifying enzymes. Proc Natl Acad Sci U S A.
Zick, M., Rabl, R., and Reichert, A.S. (2009). Cristae formation-linking ultrastructure and function of mitochondria. Biochim Biophys Acta 1793, 5-19.
Zingaretti, M.C., Crosta, F., Vitali, A., Guerrieri, M., Frontini, A., Cannon, B., Nedergaard, J., and Cinti, S. (2009). The presence of UCP1 demonstrates that metabolically active adipose tissue in the neck of adult humans truly represents brown adipose tissue. FASEB J 23, 3113-3120.

Figure Legends:

Figure 1. Tyk2-/- mice develop metabolic abnormalities.
A) Mice pictured at 12 months of age. **B)** Body weight of mice fed a normal chow diet at 16 weeks of age (n = 5-8 mice per group. **C)** Glucose tolerance test in Tyk2+/+ and Tyk2-/- mice. 16 week old mice were fasted for 16 h and injected intraperitoneally (IP) with 2 mg glucose/g body weight. Blood was collected from the tail vein and glucose was measured at the indicated times (n = 5-8 mice per group). **D)** Tyk2 RNA levels in BAT and skeletal muscle (SKM) are decreased in mice on a HFD. 5 week old mice were placed on a normal chow or HFD for 12 weeks and RNA was harvested from BAT, SKM, WAT and liver. RNAs corresponding to Tyk2, Jak1 and Jak2 were measured by qPCR (n = 5 mice per group). **E)** Tyk2 RNA levels are decreased in muscle samples from obese patients with or without T2D (n = 10-15 subjects per group). **F)** BAT-specific RNAs (UCP1, PRDM16 and Cidea) are decreased in interscapular BAT isolated from 16 week old Tyk2-/- mice**.** RNAs highly expressed in BAT (PPARγ and PGC1α) are not significantly changed in BAT isolated from Tyk2-/- mice (n=5-8 mice per group). **G)** The amounts of BAT-selective proteins are decreased in Tyk2-/- mice. Cell extracts from BAT of individual Tyk2+/+ and Tyk2-/- mice were analyzed by western blotting for the presence of PRDM16, PPARγ, PPARα, Cidea and UCP1 (n=5-8 mice per group). Intensity of signals were quantified by Image J software and presented in the table. All samples were normalized to tubulin. The values represent mean fold decrease ± SE over Tyk2+/+ set as 1. **H)** H&E staining of BAT from 16 week old Tyk2+/+ and Tyk2-/- mice (n = 4 mice per group). **I)** Oxygen consumption rates measured for isolated brown adipose tissue mitochondria are reduced in Tyk2-/- mice. Mitochondria were incubated under conditions described in the Materials and Methods section. Data represent 5 separate experiments. **J)** UCP1 RNA in BAT is elevated in Tyk2+/+ but not Tyk2-/- mice upon cold exposure. Mice were placed at 4^0C for 12 hrs prior to collection of RNA from BAT (n = 5 mice per group). **K)** Body temperatures measured with a rectal thermometer in Tyk2+/+ and Tyk2-/- mice placed at 4^0 C (n = 5 mice per group).

Figure 2. Expression of Tyk2 and Stat3 are required for differentiation of brown adipocytes. A) Expression of Tyk2 or CAStat3 in immortalized Tyk2-/- preadipocytes restores lipid accumulation. Cell lines were subjected to *in vitro* differentiation and stained with working solution of Oil red O. **B)** Stat3 protein level in Tyk2+/+ preadipocytes infected with shRNA directed against Stat3 or a scrambled control (SCR). **C)** Amount of brown adipose tissue-specific (UCP1, Cidea) and adipogenic (PPARγ, aP2) RNAs in Stat3 shRNA or SCR control shRNA expressing adipocytes (n = 4 independent experiments).

Table 1. Reduced gene expression in Tyk2 deficient adipocytes is restored by reconstitution with CAStat3 and partially with Tyk2. Total RNA was isolated from in vitro differentiated adipocytes and analyzed for selected RNA levels using qPCR. The values represent mean fold change ± SE over Tyk2+/+ set as 1, for n = 5 independent experiments.

Figure 3. PRDM16 and Stat3 regulate differentiation of brown preadipocytes. A) Oil red O staining of immortalized brown adipocytes expressing indicated retroviral vectors 5 days after inducing adipocyte differentiation (n = 3 independent experiments). **B)** Stat3 coimmunoprecipitates with PRDM16. Cell extracts prepared from differentiated Tyk2-/- adipocytes expressing PRDM16 or PRDM16 and C/EBPβ were immunoprecipitated with either IgG (lanes 1 and 3) or PRDM16 (lanes 2 and 4) antisera. The immunoblots were probed for either PRDM16 or Stat3. Endogenous Stat3 was detected in the complex with PRDM16 by western blotting. Input is shown in the lower panels. IB-immunoblot, IP-immunoprecipitate (n = 3 independent experiments). **C)** The same cell extracts used in panel B were immunoprecipitated with either IgG or Stat3 antisera. The immunoblots were probed for either PRDM16 or Stat3. Input is shown in the lower panels (n = 3 independent experiments). **D)** Cell extracts from differentiated wild type brown adipocytes were

immunoprecipitated with either IgG or Stat3 antisera. The immunoblots were probed for either PRDM16 or Stat3. Input is shown in the lower panels (n = 2 independent experiments). **E)** Stat3-/- adipocytes are insensitive to rosiglitazone induced accumulation of PRDM16. Cell lines were generated from immortalized Floxed Stat3+/+ preadipocytes infected with a retrovirus expressing Cre recombinase or an empty vector control. Cell lines were differentiated in the presence or absence of rosiglitazone (1μM). Extracts were western blotted for the expression of PRDM16, Stat3 and tubulin as a control for protein loading (n = 4 independent experiments). **F)** The same Stat3+/+ and Stat3-/- cell lines were incubated with or without rosiglitazone (1μM) for 4 days (non-differentiating conditions). Protein extracts western blotted for the expression of PRDM16, Stat3 and tubulin as a control for protein loading (n = 3 independent experiments) **G)** Stat3 expression does not affect cellular levels of PRDM16 RNA. Cells were exposed to rosiglitazone as described in C). RNA was harvested and PRDM16 transcripts were measured by qPCR (n = 4 independent experiments).

Table 2. Reconstitution of brown adipose tissue-specific gene expression in Tyk2-/- preadipocytes through PRDM16 and C/EBPβ. Total RNA was isolated from in vitro differentiated adipocytes and analyzed for selected RNA levels. The values represent mean fold change ± SE over Tyk2+/+ set as 1, for n = 4 independent experiments.

Figure 4. Expression of CAStat3 in BAT reverses obesity in Tyk2-/- mice. A) The BAT-specific RNA levels (UCP1, PRDM16, Cidea) and highly expressed BAT RNA expression (PPARγ, C/EBPβ, PPARα) are restored in tissue from Tyk2-/- mice that express the CAStat3 transgene. Total RNA was isolated from interscapular BAT of 12 week old mice (n = 6-8 mice per group). **B)** The amounts of BAT-enriched proteins are increased in CAStat3 mice. Cell extracts from BAT of individual CTR and CAStat3 mice were analyzed by western blotting for the presence of PRDM16, PPARα, PPARγ, Cidea and UCP1 (n=6-8 mice per group). Intensity of signals were quantified by Image J software and presented in the table. All samples were normalized to tubulin. The values represent mean fold increase ± SE over CTR mice set as 1. **C)** H&E staining of interscapular BAT from 12 week old control (CTR) and CAStat3 expressing mice (n = 5 mice per group). **D)** Body weight of 24 week old CAStat3 and control mice fed a regular chow diet (n = 10-12 mice per group). **E)** Fasted plasma insulin levels of 24 week old control and CAStat3 expressing mice (n = 10-12 mice per group).

Fig. 1A

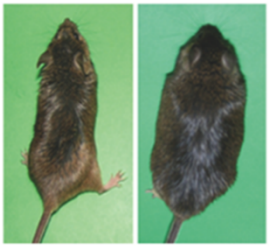

Fig. 1B

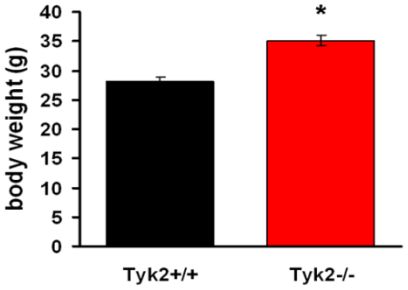

Fig. 1C

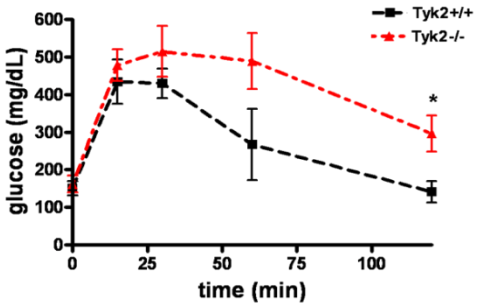

Fig. 1D

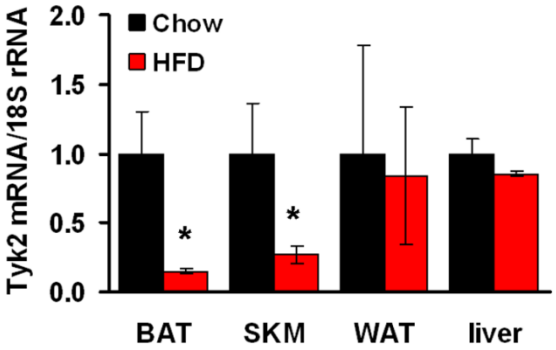

Fig. 1E

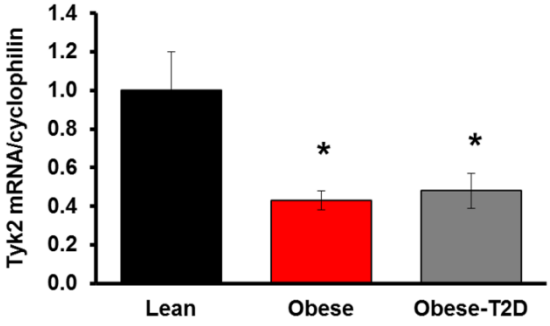

Fig. 1F

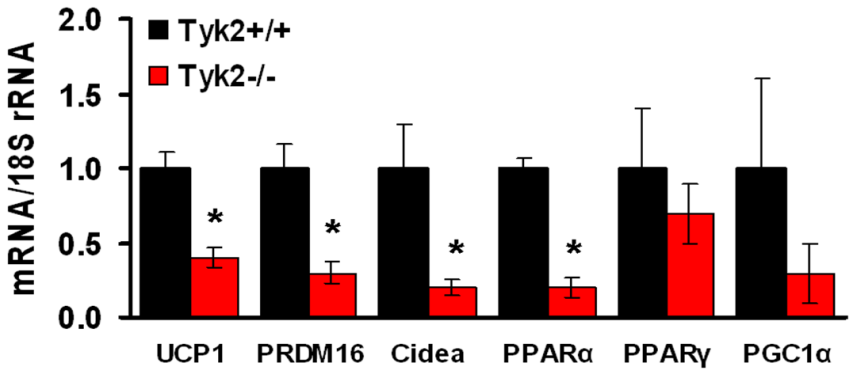

Fig. 1G

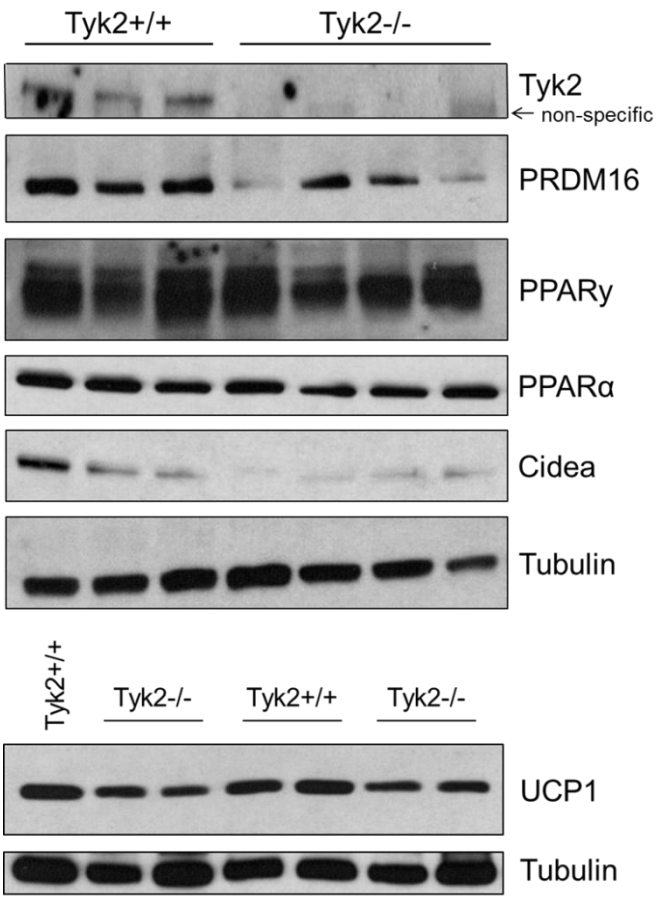

	Tyk2+/+	Tyk2-/-
PRDM16	1	0.5 ± 0.1 *
PPARγ	1	1.2 ± 0.2 *
PPARα	1	0.8 ± 0.08 *
Cidea	1	0.2 ± 0.04 *
UCP1	1	0.7 ± 0.05 *

Fig. 1H

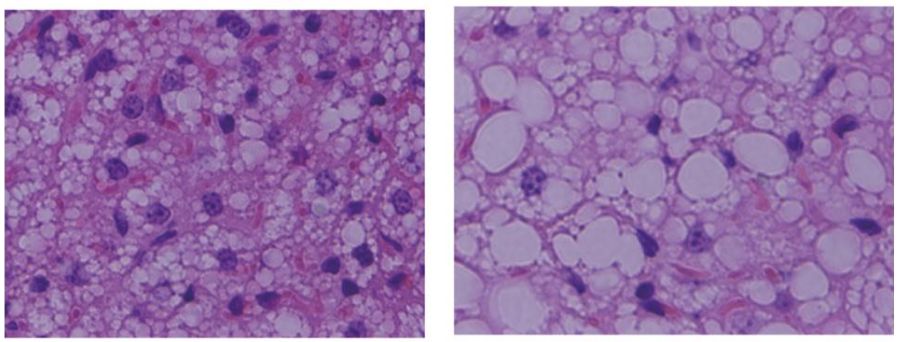

Tyk2+/+ **Tyk2-/-**

Fig. 1I

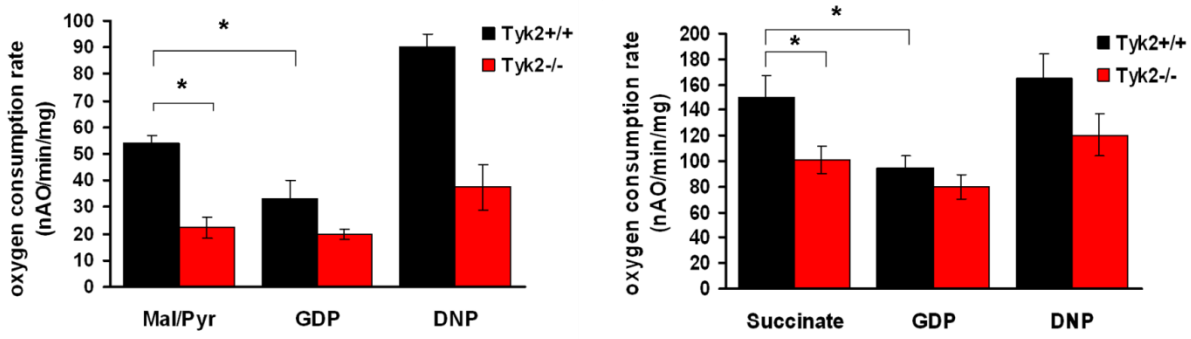

Fig. 1J

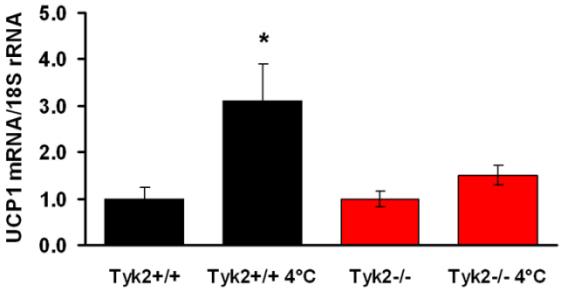

Fig. 1K

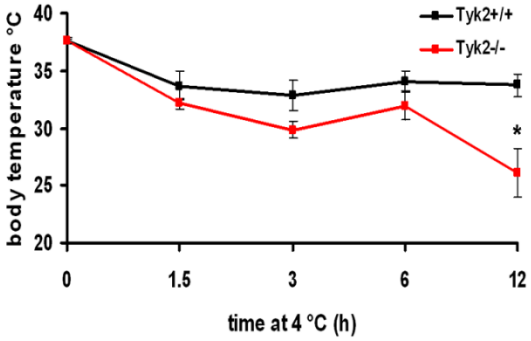

Fig. 2A

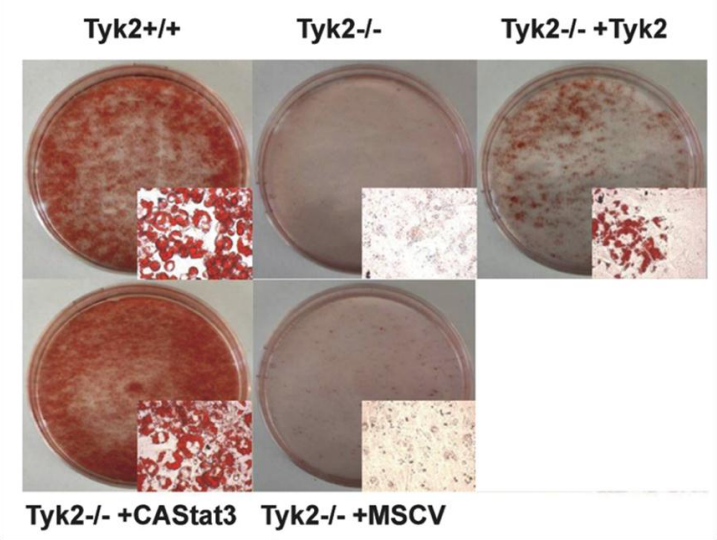

Table 1.

	Tyk2+/+	Tyk2-/-	Tyk2-/- +MSCV	Tyk2-/- +Tyk2	Tyk2-/- +CAStat3
UCP1	1	0.1 ± 0.03 *	0.1 ± 0.04 *	0.5 ± 0.1	1.3 ± 0.4
PRDM16	1	0.1 ± 0.04 *	0.2 ± 0.07 *	0.3 ± 0.09 *	1.1 ± 0.4
Cidea	1	0.2 ± 0.07 *	0.2 ± 0.07 *	0.4 ± 0.2 *	2.3 ± 0.6
Elovl3	1	0.3 ± 0.17 *	0.5 ± 0.2 *	0.6 ± 0.4 *	1.5 ± 0.5
PGC1α	1	0.1 ± 0.02 *	0.1 ± 0.02 *	0.2 ± 0.09 *	1.7 ± 0.7
PPARα	1	0.3 ± 0.1 *	0.3 ± 0.04 *	0.2 ± 0.08 *	1.2 ± 0.6
PPARγ	1	0.2 ± 0.05 *	0.2 ± 0.06 *	0.3 ± 0.07 *	1.8 ± 0.4
MCK	1	8.4 ± 2.0 *	6.3 ± 1.4 *	2.7 ± 0.5	3.4 ± 0.5 *
MyoD	1	7.5 ± 1.7 *	10 ± 2.2 *	2.9 ± 0.5	4.3 ± 0.7 *
Myg	1	12 ± 2.1 *	29 ± 1.3 *	2.6 ± 0.2	3.5 ± 1.7

Fig. 2B

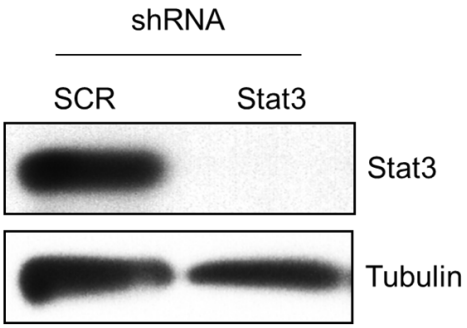

Fig. 2C

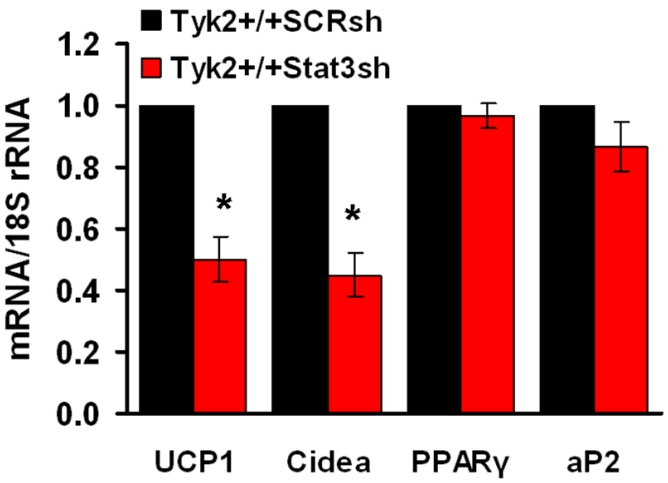

Fig. 3A

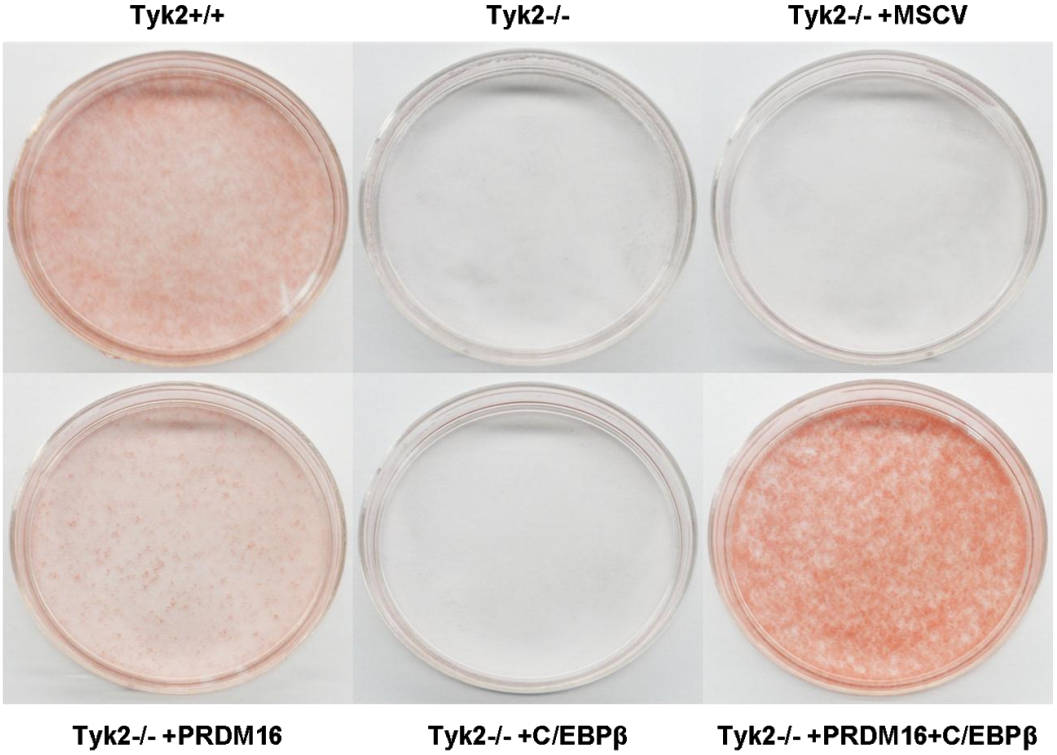

Table 2.

	Tyk2+/+	Tyk2-/-	Tyk2-/- +MSCV	Tyk2-/- +PRDM16	Tyk2-/- +C/EBPβ	Tyk2-/- +PRDM16 +C/EBPβ
UCP1	1	0.2 ± 0.09 *	0.2 ± 0.1 *	1.4 ± 0.35	0.1 ± 0.7 *	1.1 ± 0.08
PRDM16	1	0.2 ± 0.07 *	0.3 ± 0.1 *	760 ± 84	0.2 ± 0.03 *	1150 ± 307
Cidea	1	0.1 ± 0.03 *	0.1 ± 0.03 *	0.45 ± 0.1 *	0.1 ± 0.04 *	2.9 ± 0.3
Elovl3	1	0.2 ± 0.09 *	0.2 ± 0.1 *	0.2 ± 0.05 *	0.3 ± 0.1 *	2.1 ± 0.6
PGC1α	1	0.1 ± 0.02 *	0.1 ± 0.03 *	0.5 ± 0.15 *	0.2 ± 0.06 *	2.7 ± 0.8
PPARα	1	0.3 ± 0.2 *	0.3 ± 0.2 *	0.95 ± 0.15	0.4 ± 0.2 *	1.0 ± 0.1
PPARγ	1	0.2 ± 0.09 *	0.2 ± 0.04 *	0.4 ± 0.1 *	0.3 ± 0.1 *	1.2 ± 0.4

Fig. 3B

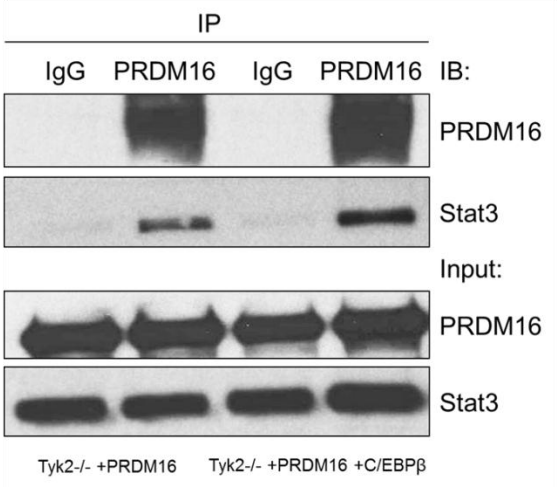

Fig. 3C

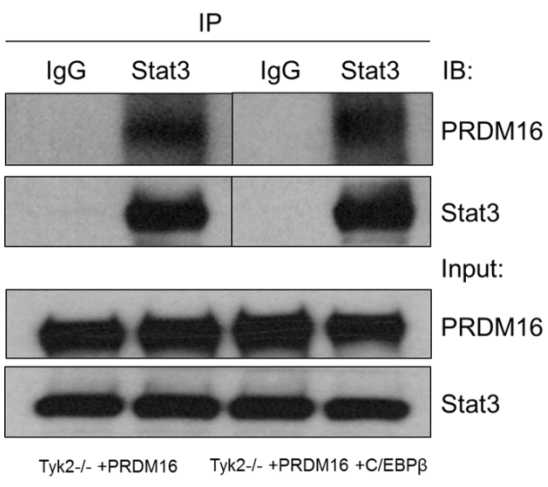

Fig. 3D

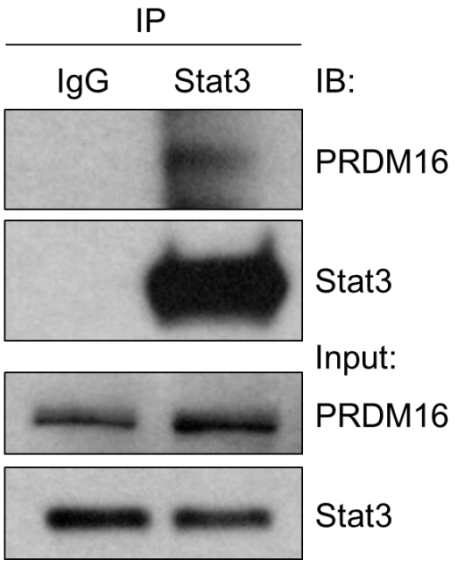

Fig. 3E

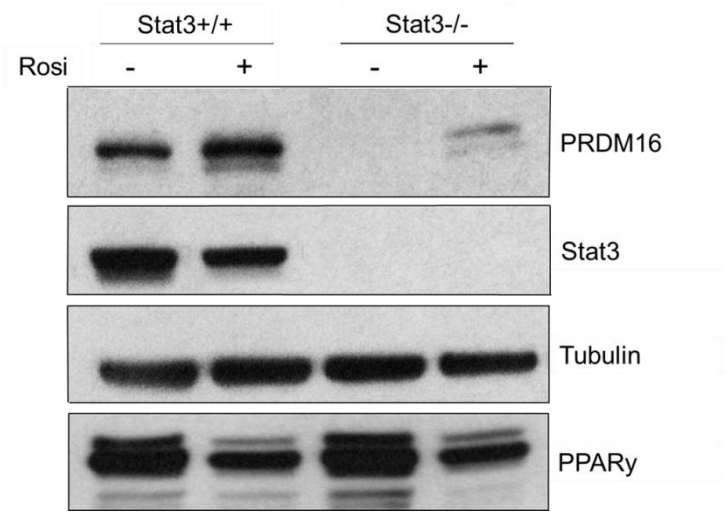

Fig. 3F

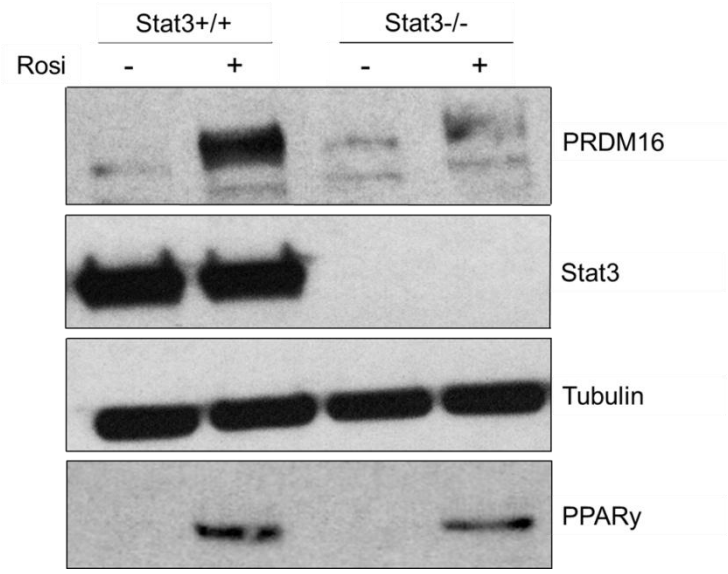

Fig. 3G

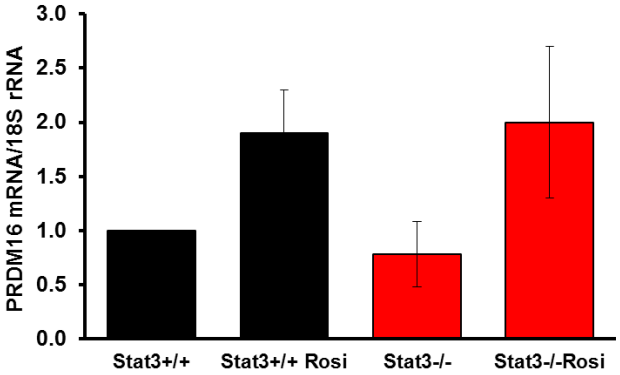

Fig. 4A

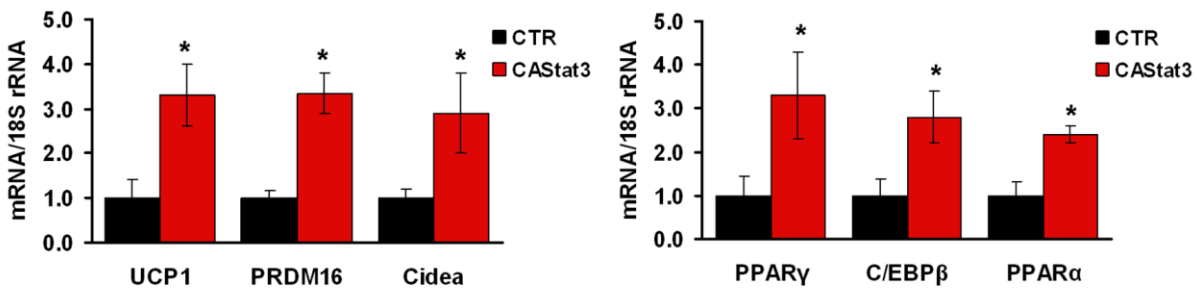

Fig. 4B

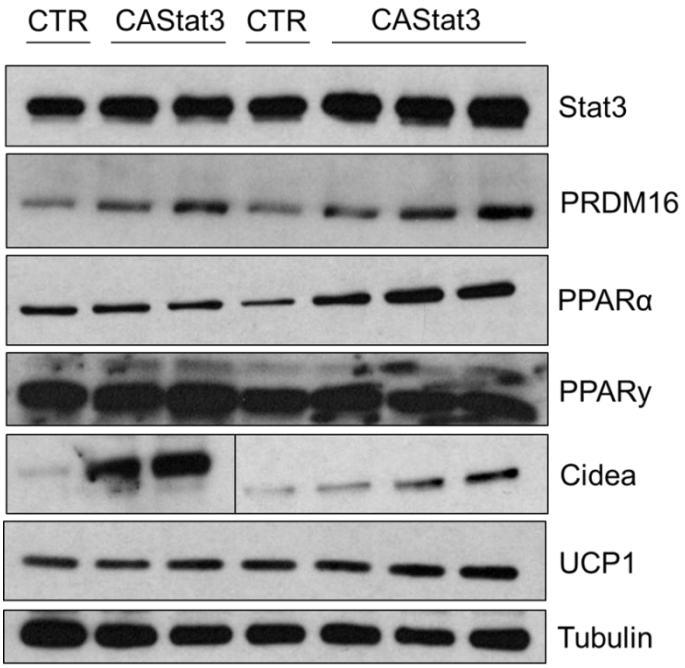

	CTR	CAStat3
PRDM16	1	2.2 ± 0.2 *
PPARα	1	2.0 ± 0.2 *
PPARγ	1	0.7 ± 0.2
Cidea	1	5.9 ± 3 *
UCP1	1	1.6 ± 0.2
Stat3	1	1.1 ± 0.2

Fig. 4C

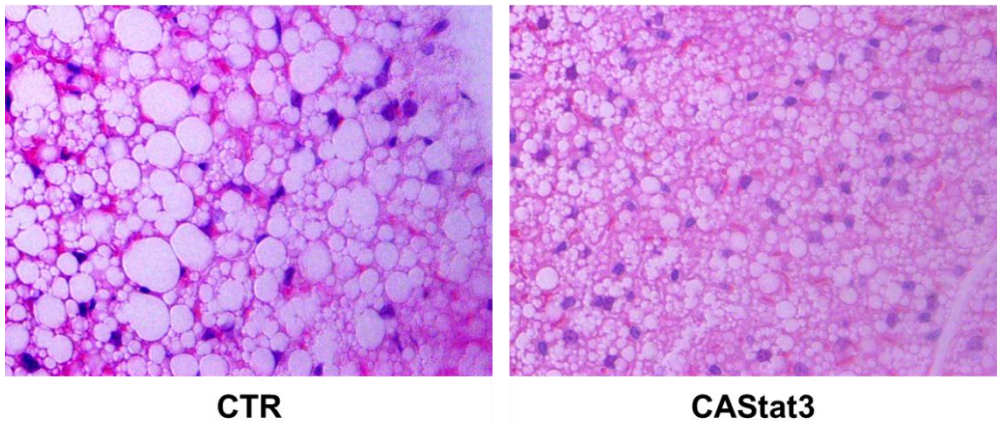

Fig. 4D

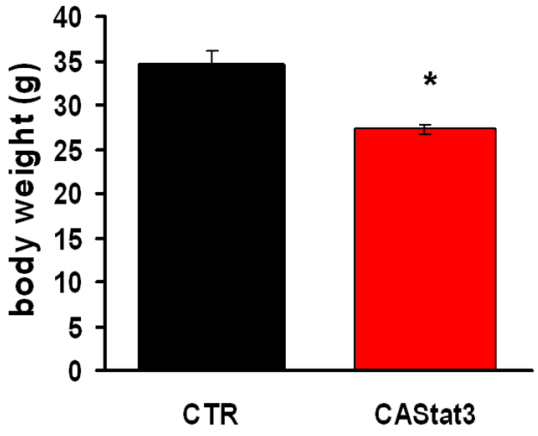
body weight (g)
40
35
30
25
20
15
10
5
0
*
CTR
CAStat3

Fig. 4E

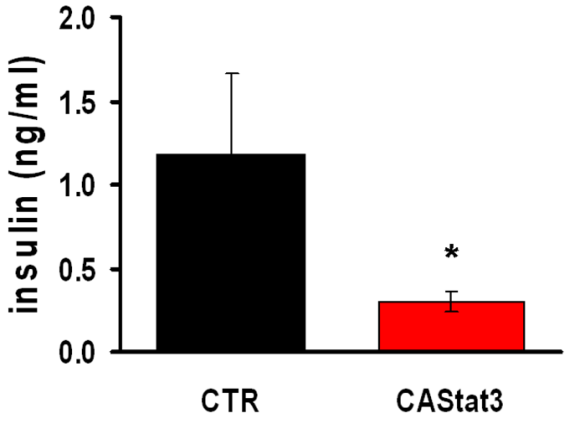
insulin (ng/ml)
2.0
1.5
1.0
0.5
0.0
*
CTR
CAStat3

Supplemental Figure Legends

Table S1. Metabolic analysis of Tyk2+/+ and Tyk2-/- mice. The parameters were determined from plasma taken via heart puncture from mice fasted for 16 h (n = 3 mice per group).

Figure S1. Analysis of energy expenditure. Energy expenditure was measured for 24 hrs in individually housed 12 week old Tyk2+/+ and Tyk2-/- mice (n = 6 mice per group). All measured parameters are normalized by lean body mass (LBM). Energy expenditure is reported as **A)** VO_2 consumption, **B)** VCO_2 production, **C)** heat production, **D)** RNA levels of β-oxidation enzymes (LCAD and AOX) are decreased in BAT isolated from 20 week old Tyk2-/- mice (n=5-10 mice per group).

Figure S2. Analysis of Tyk2, Jak1 and Jak2 mRNA and Tyk2 protein in tissues from Tyk2+/+ and Tyk2-/- mice subjected to high fat diet (HFD) and skeletal muscle form obese and lean humans. A) Tyk2 protein levels were analyzed by western blotting in BAT, SKM, sWAT (subcutaneous), vWAT (visceral), liver and spleen isolated from C57BL/6 mice (n = 3 mice per group). 5 week old C57BL/6 mice were placed on a normal chow or HFD for 12 weeks. Tissue extracts and RNA were harvested from BAT, SKM, WAT and liver. **B)** Tyk2 protein level is decreased in BAT in mice fed HFD (n = 6 mice per group). **C)** Jak1 RNA and **D)** Jak2 RNA were measured by qPCR (n = 5 mice per group). **E)** Tyk2, Jak1 and Jak2 expression in BAT from 12 week old control (CTR) and ob/ob mice fed with normal chow diet (n = 5 mice per group). **F)** Jak1 and Jak2 RNA levels in skeletal muscle obtained from lean controls and obese patients with or without diabetes (n = 10-15 subjects per group).

Figure S3. Changes in mitochondrial morphology in BAT and skeletal muscle of Tyk2-/- mice. A) Representative electron microscopy micrographs from BAT, SKM and heart of Tyk2+/+ and Tyk2-/- mice (n = 6 mice per group). The expression level of **B)** OPA1, **C)** Mfn1 and **D)** Mfn2 in BAT, SKM, WAT and liver of 12-week-old Tyk2+/+ and Tyk2-/- mice (n = 6-8 mice per group).

Figure S4. DNA methylation is decreased and accumulation of histone activation marks are increased in the UCP1 and Cidea promoters in Tyk2+/+ compared with Tyk2-/- adipocytes. A) Cidea and UCP1 promoters show increased methylation in Tyk2-/- cells. Bisulphite sequencing of CpGs was carried out after isolation of genomic DNA from Tyk2+/+ and Tyk2-/- preadipocytes. Black and white circles indicate methylated and unmethylated CpGs, respectively. The red frames indicate CpGs overlapping with C/EBPβ binding sites. The Cidea promoter contains 44 CpGs (-550 to +250b). The UCP1 promoter contains 30 CpGs (-500 to +200b).
Chromatin immunoprecipitaion (ChIP) assays were performed using immortalized and in vitro differentiated Tyk2+/+ and Tyk2-/- adipocytes. Cross-linked chromatin was immunoprecipitated with antisera that recognizes H3K4me3 or nonspecific IgG. The immunoprecipitates were subjected to qPCR using primers corresponding to **B)** the UCP1 promoter or **C)** the Cidea promoter. **D)** As a control to demonstrate that the decreased binding of H3K4me3 to these promoters in Tyk2-/- cells was not a global effect on all transcription units, we also measured binding of H3K4me3 to the p16 promoter which is not altered by the lack of Tyk2 expression. Data represent four independent experiments.

Table S1

	3 months		12 months	
	Tyk2+/+	Tyk2-/-	Tyk2+/+	Tyk2-/-
Glucose (mg/dL)	92.3 ± 4.9	92.2 ± 4.7	76.2 ± 3.7	79.0 ± 3.5
Insulin (µg/L)	0.16 ± 0.14	0.63 ± 0.15 *	0.17 ± 0.21	0.64 ± 0.60 *
Triglyceride (mg/dL)	48.6 ± 7.5	47.0 ± 5.8	57.0 ± 3.2	98.6 ± 20.2
FFA (mM)	0.58 ± 0.14	0.71 ± 0.02	0.68 ± 0.11	0.99 ± 0.07
Cholesterol (mg/dL)	119.7 ± 6.7	99.67 ± 12.44	122.8 ± 5.2	154.0 ± 2.9 *
β-Hydroxybutyrate (mM)	1.11 ± 0.10	0.60 ± 0.16	0.74 ± 0.053	0.68 ± 0.11

Fig. S1A

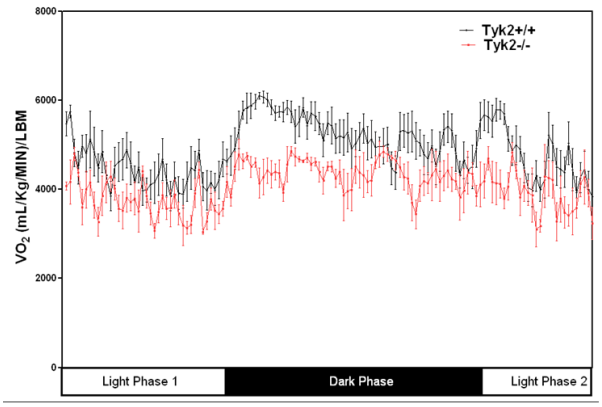

Fig. S1B

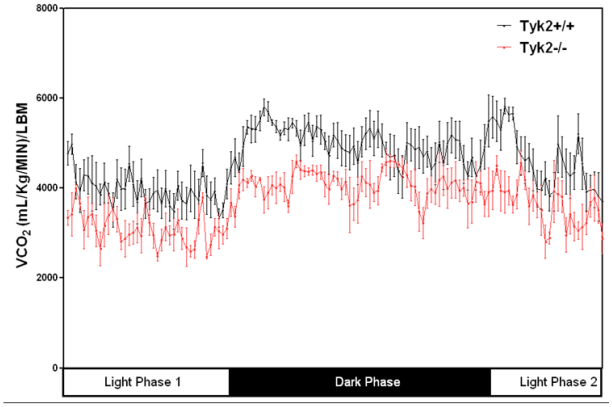

Fig. S1C

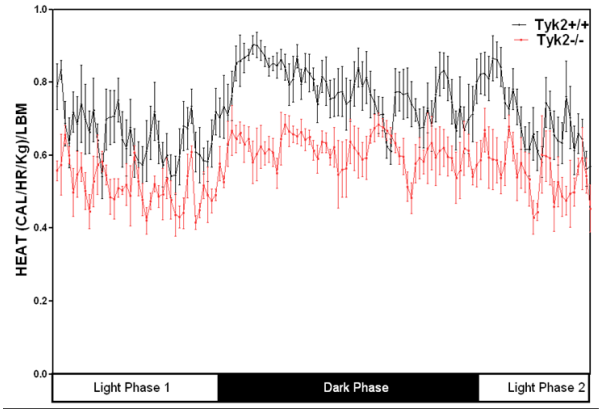

Fig. S1D

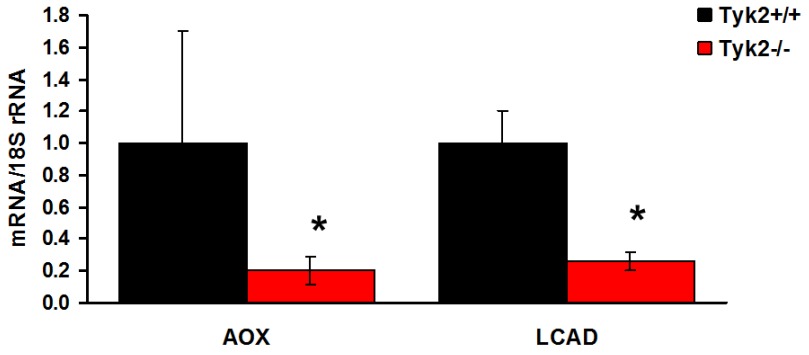

Fig. S2A

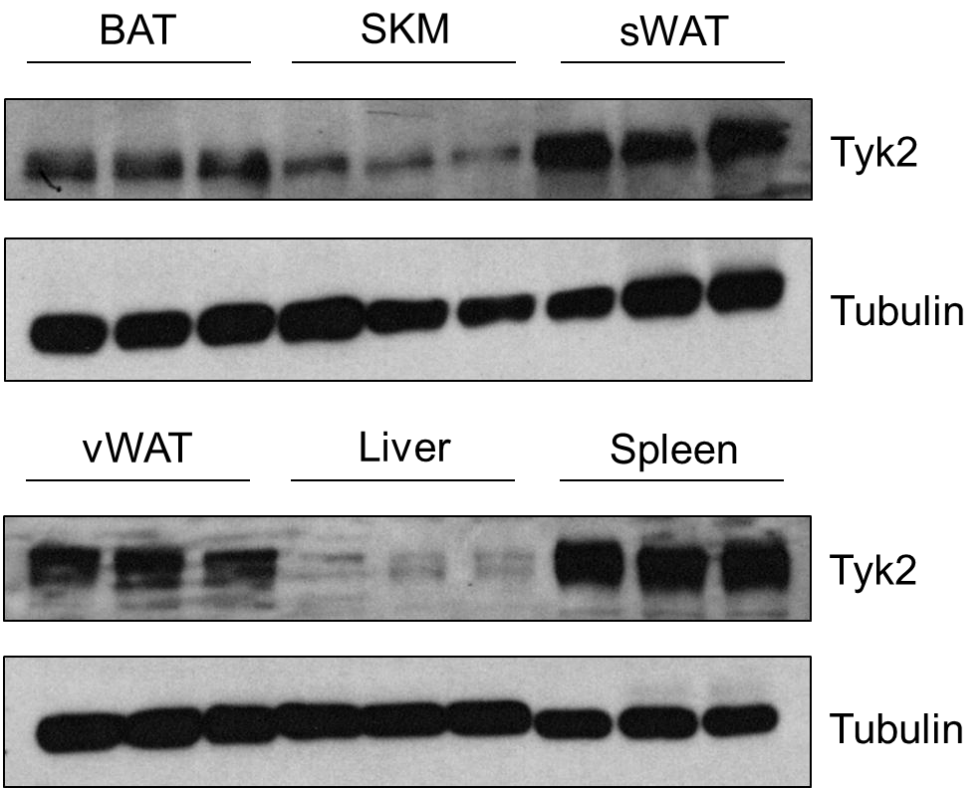

Fig. S2B

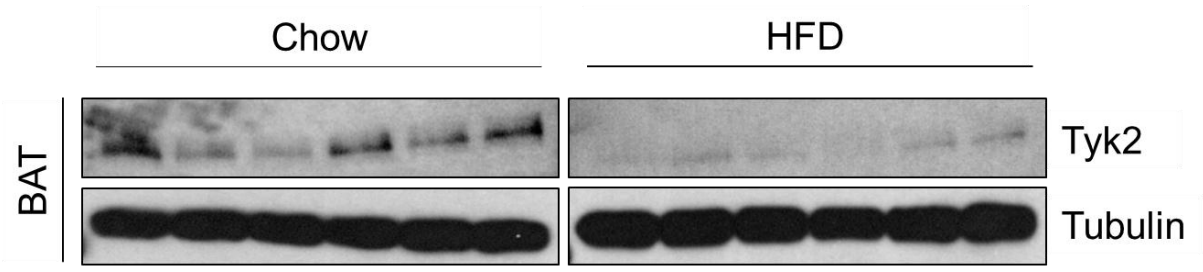

Fig. S2C

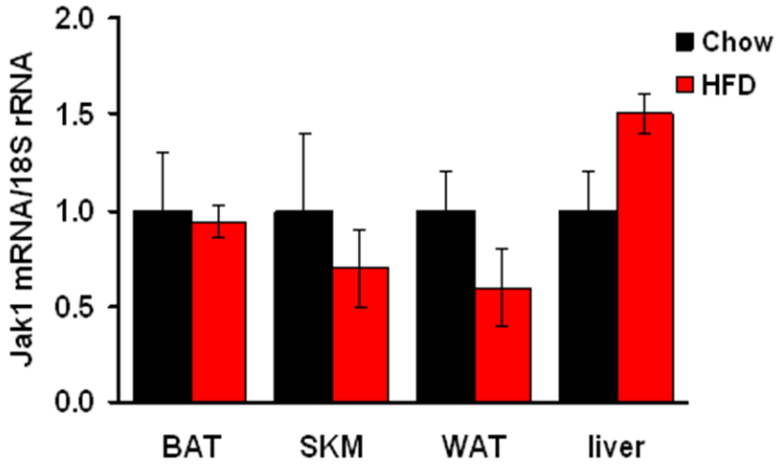

Fig. S2D

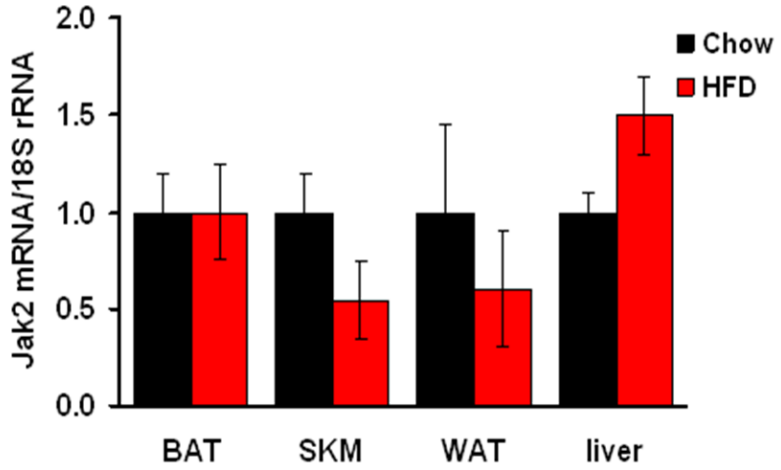

Fig. S2E

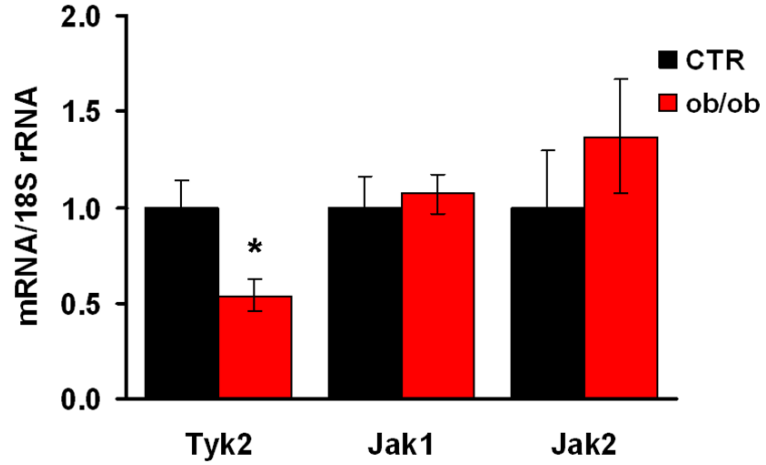

Fig. S2F

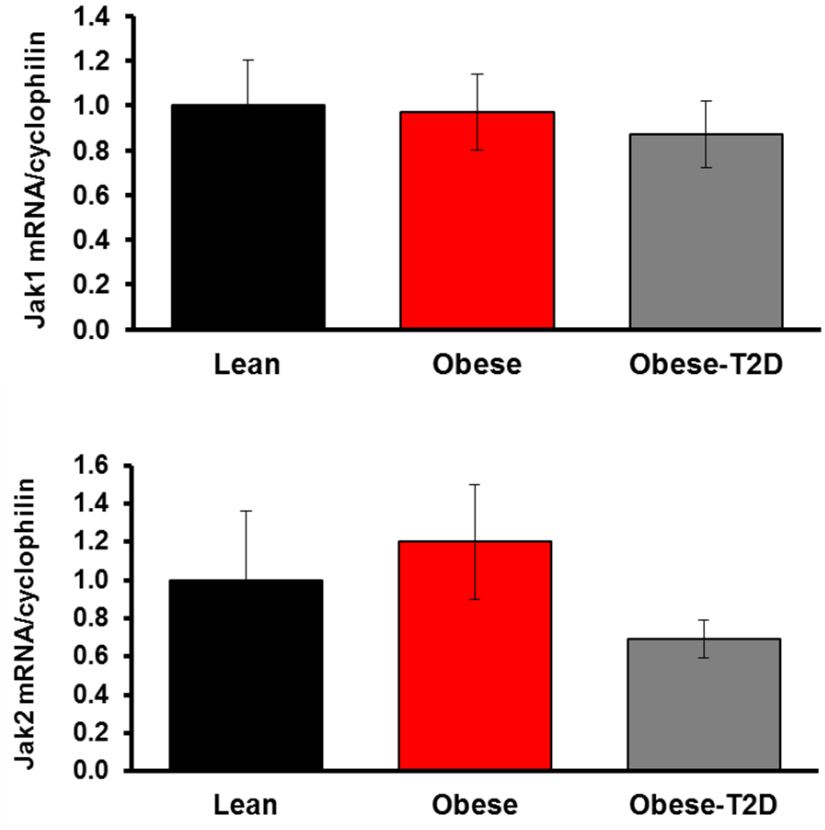
Jak1 mRNA/cyclophilin
1.4
1.2
1.0
0.8
0.6
0.4
0.2
0.0
Lean
Obese
Obese-T2D
Jak2 mRNA/cyclophilin
1.6
1.4
1.2
1.0
0.8
0.6
0.4
0.2
0.0
Lean
Obese
Obese-T2D

Fig. S3A

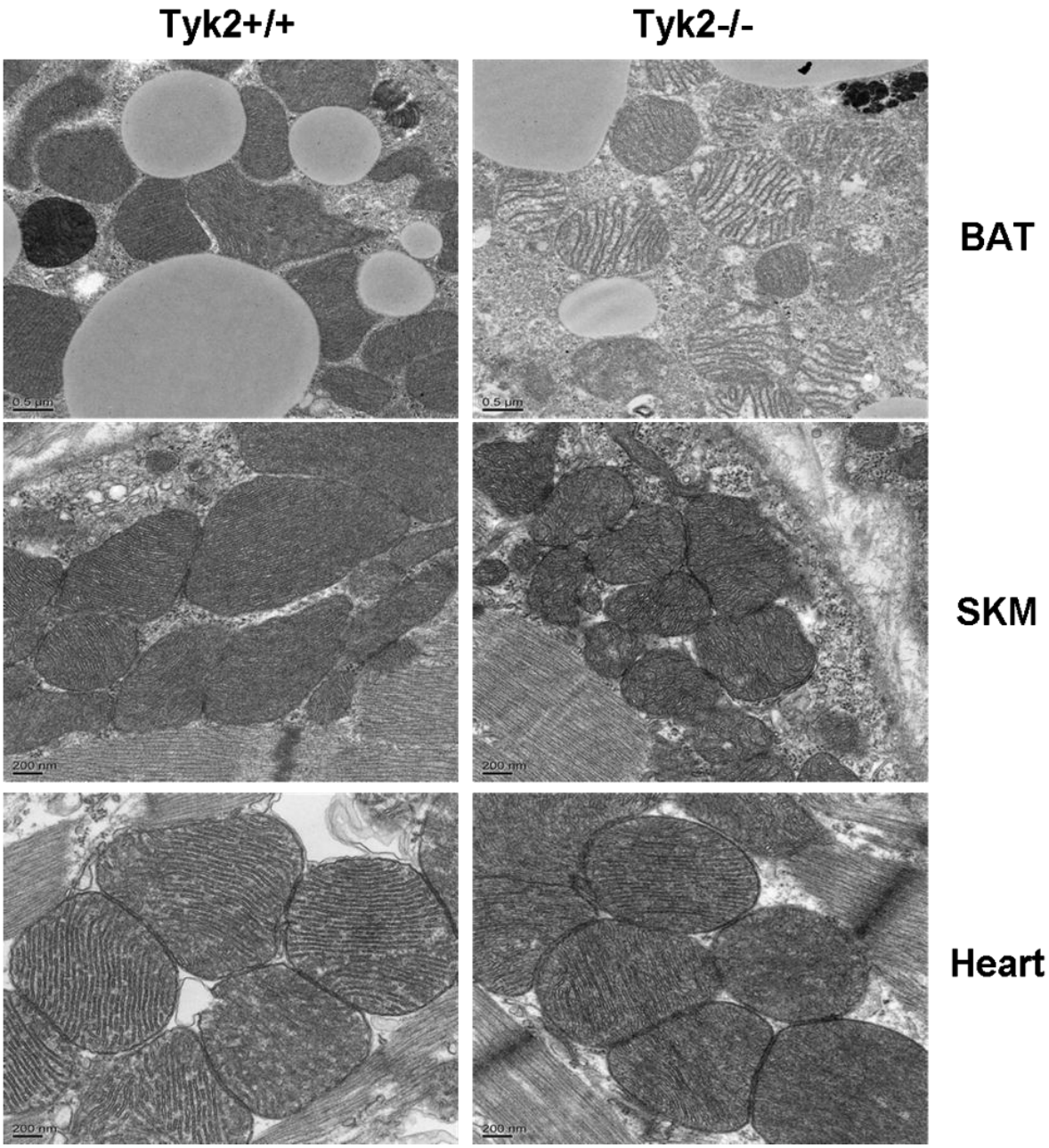

Fig. S3B

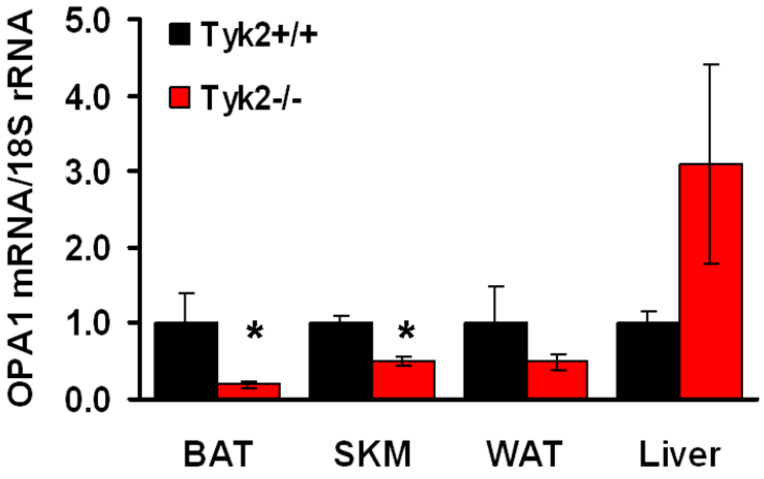

Fig. S3C

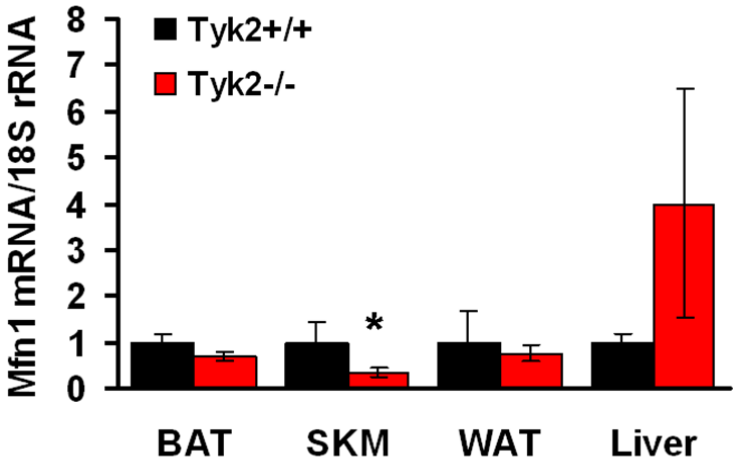

Fig. S3D

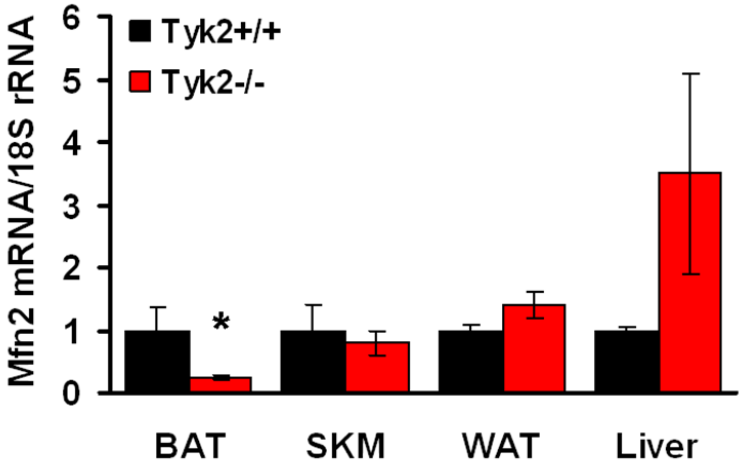

Fig. S4A

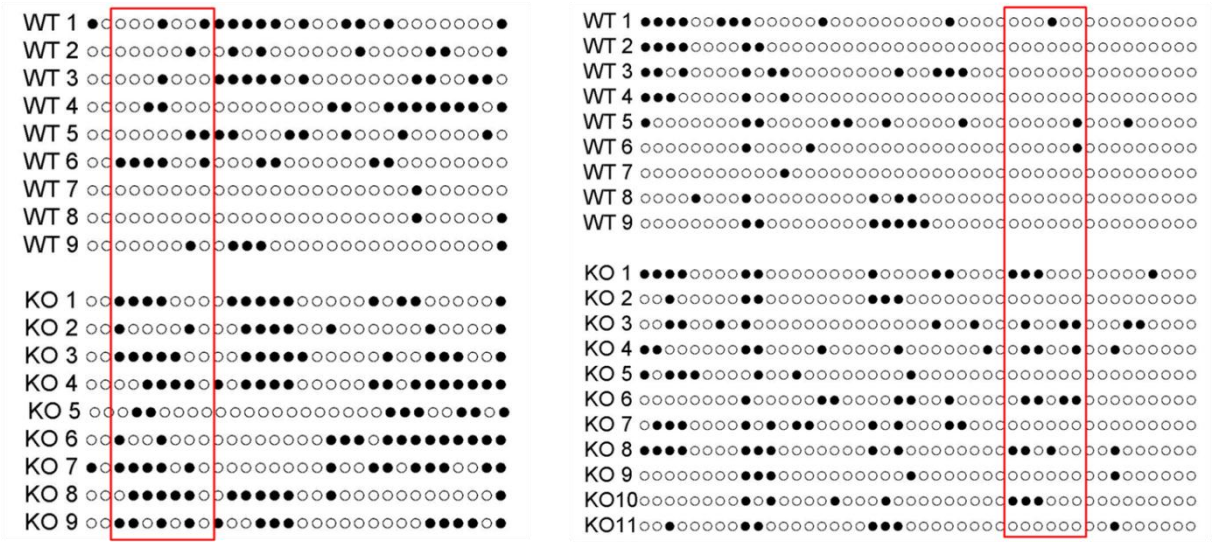

Fig. S4B

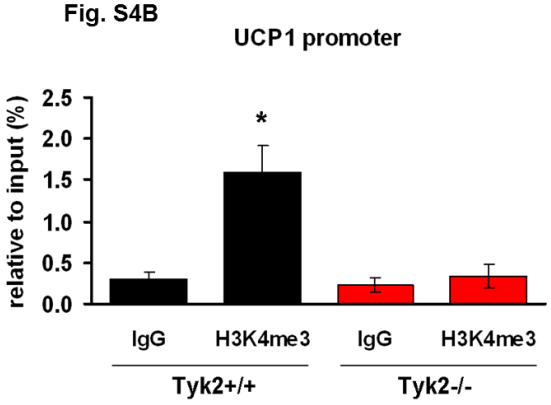

Fig. S4C

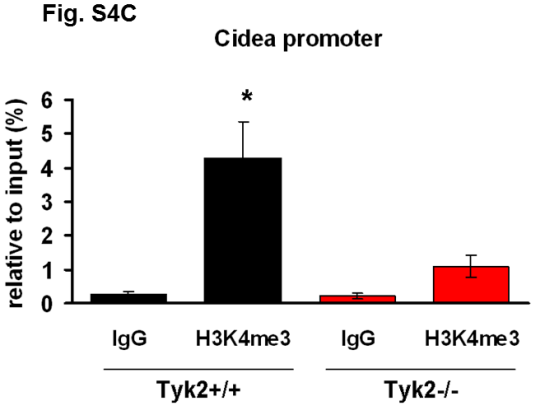

Fig. S4D

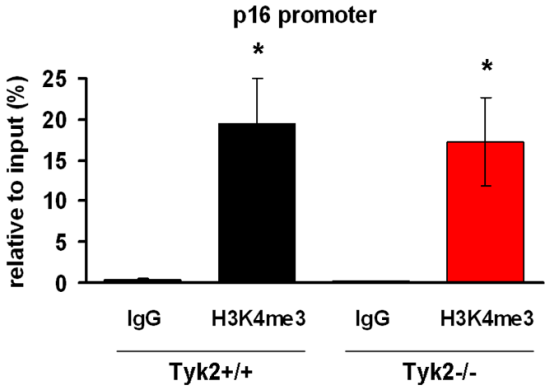

Table S2. Real-time qPCR primer sequences.

Gene	Primer sequence
UCP1	(F) 5’- CTGGGCTTAACGGGTCCTC -3’ (R) 5’- CTGGGCTAGGTAGTGCCAGTG -3’
PRDM16	(F) 5’- CAGCACGGTGAAGCCATTC -3’ (R) 5’- GCGTGCATCCGCTTGTG -3’
Cidea	(F) 5’- TGCTCTTCTGTATCGCCCAGT -3’ (R) 5’- GCCGTGTTAAGGAATCTGCTG -3’
Elovl3	(F) 5’- TCCGCGTTCTCATGTAGGTCT -3’ (R) 5’- GGACCTGATGCAACCCTATGA -3’
PGC1α	(F) 5’- CCCTGCCATTGTTAAGACC -3’ (R) 5’- TGCTGCTGTTCCTGTTTTC -3’
PPARα	(F) 5’- GCGTACGGCAATGGCTTTAT -3’ (R) 5’- GAACGGCTTCCTCAGGTTCTT -3’
PPARγ	(F) 5’- GTGCCAGTTTCGATCCGTAGA -3’ (R) 5’- GGCCAGCATCGTGTAGATGA -3’
C/EBPβ	(F) 5’- AAGAGCCGCGACAAGGC -3’ (R) 5’- GTCAGCTCCAGCACCTTGTG -3’
AOX	(F) 5’- AAGAGTTCATTCTCAACAGCCC -3’ (R) 5’- CTTGGACAGACTCTGAGCTGC -3’
LCAD	(F) 5’- GCTGCCCTCCTCCCGATGTT -3’ (R) 5’- ATGTTTCTCTGCGATGTTGATG -3
aP2	(F) 5’- ACACCGAGATTTCCTTCAAACTG -3’ (R) 5’- ACACCGAGATTTCCTTCAAACTG -3’
MCK	(F) 5’- GCAAGCACCCCAAGTTTGA -3’ (R) 5’- ACCTGTGCCGCGCTTCT -3’
Myg	(F) 5’- AGCGCAGGCTCAAGAAAGTGAATG -3’ (R) 5’CTGTAGGCGCTCAATGTACTGGAT -3’
MyoD	(F) 5’- CGCCACTCCGGGACATAG -3’ (R) 5’- GAAGTCGTCTGCTGTCTCAAAGG -3’
18S rRNA	(F) 5’- CCATCCAATCGGTAGTAGCG -3’ (R) 5’- GTAACCCGTTGAACCCCATT -3’
human Tyk2	(F) 5’-GGGACCGTGGGCAGGAGCTA-3’ (R) 5’-GTGCGTGTGGGAGACCTGGC-3’

human Jak1	(F) 5’-ATTGGCGAGATCCCCTTGA-3’ (R) 5’-GCACCGGCTTTCATAGAATCTCT-3’
human Jak2	(F) 5’-TGATTTTGTGCACGGATGGA-3’ (R) 5’-ACTGCCATCCCAAGACATTCTT-3’
human Cyclophilin A	(F) 5’-CATCTGCACTGCCAAGACTGA -3’ (R) 5’-GCAAAGTGAAAGAAGGCATGAA- 3’

Table S3. Bisulfite-specific primer sequences.

Promoter	Primer sequence
Cidea	(F) 5’- GTTTAGTTATTAATGGGTGGTACTATT -3' (R) 5’- AAAACACTCCACTAAACACCTATAAC -3'
UCP1	(F) 5’- GAAAGGGATATTTAGAATTGAAAGGAG -3’ (R) 5’- CTACCAACAAACTAAAACTCCGAC -3’

Table S4. ChIP primer sequences.

Promoter	Primer sequence
Cidea	(F) 5’- GAGGTTCCTCCCGAAAAAGG -3’ (R) 5’- CAACAGAATGAGGGCACCC -3’
UCP1	(F) 5’- GCACTCACGCCTCTCTGC -3’ (R) 5’- CCTCATCAATGTCACTAACTC -3’
p16	(F) 5’- ACACTCCTTGCCTACCTGAA -3’ (R) 5’- CGAACTCGAGGAGAGCCATC -3’